File

I.O.S.

INSTITUTE OF OCEANOGRAPHIC SCIENCES

SOME LABORATORY MEASUREMENTS ON AN ACOUSTIC CURRENT METER DEVELOPED AT CHRISTIAN MICHELSEN INSTITUTE, NORWAY

by

P. G. COLLAR and T. J. P. GWILLIAM

REPORT No. 47

1977

NATURAL ENVIRONMENT RESEARCH COUNCIL

INSTITUTE OF OCEANOGRAPHIC SCIENCES

INSTITUTE OF OCEANOGRAPHIC SCIENCES

Wormley, Godalming,
Surrey, GU8 5UB.
(0428 - 79 - 4141)

(Director: Professor H. Charnock)

Bidston Observatory,
Birkenhead,
Merseyside, L43 7RA.
(051-653-8633)

(Assistant Director: Dr. D. E. Cartwright)

Crossway,
Taunton,
Somerset, TA1 2DW.
(0823-86211)

(Assistant Director: M. J. Tucker)

Marine Scientific Equipment Service
Research Vessel Base,
No. 1 Dock.
Barry,
South Glamorgan, CF6 6UZ.
(0446-737451)
(Officer-in-Charge: Dr. L. M. Skinner)

INSTITUTE OF OCEANOGRAPHIC SCIENCES

SOME LABORATORY MEASUREMENTS ON AN ACOUSTIC CURRENT METER DEVELOPED AT CHRISTIAN MICHELSEN INSTITUTE, NORWAY

by

P.G. COLLAR and T.J.P. GWILLIAM

REPORT No. 47

1977

Institute of Oceanographic Sciences
Wormley, Godalming, Surrey, GU8 5UB

SOME LABORATORY MEASUREMENTS ON AN ACOUSTIC CURRENT METER DEVELOPED AT CHRISTIAN MICHELSEN INSTITUTE, NORWAY

1. Introduction

This report describes the results of some tests made in the IOS towing tank at Wormley on an acoustic current meter loaned by the Christian Michelsen Institute, Bergen. Norway.

This is a 'second generation' instrument, distinguished from the traditional rotor-vane types by the absence of moving parts. A description of the instrument and the principles applied in its design is given in GYTRE, 1975. These may be briefly summarized as follows.

A measurement is made of the components of flow resolved along two orthogonal axes. For each axis two facing transducers separated by distance ℓ are pulsed simultaneously. Each then receives the signal transmitted by the other. The travel time for the acoustic pulse between the transducers is dependent on the component, v, of the fluid velocity resolved along the axis as well as on the velocity of sound in still water, c. It can be shown that the fluid velocity component is given to an acceptable degree of approximation by: $v = c^2\Delta t/2\ell$ where Δt is the measured difference in transit times of upstream and downstream pulses. The velocity of sound c is dependent on temperature and a correction for this is derived by measuring pulse transit time ($\simeq c/\ell$. $v \ll c$); this is used to adjust the overall sensitivity to a constant value. The sensor has a low velocity threshold ($\sim$ 1mm/sec) determined by the time difference resolution ($\sim 10^{-10}$ sec). A relatively high bandwidth is also attainable with the method since the pulse repetition frequency can be made high. In the present sensor it was limited to 10Hz by output filters.

The appearance of the instrument loaned to the IOS is shown in Figs. 1(a) and (b). The circular transducers, approximately 1cm in diameter. are mounted on short tubular spars projecting from a central boss. Note that the acoustic path (shown by the broken line) is directed via a reflector to minimize wake effects, and that the ends of the spars are shaped to reduce the component of the spar wake along the acoustic path. This particular sensor was not self-contained, in that power was supplied externally. and a compass was not included. Voltage analogue outputs were obtained for each axis.

A number of tests have been carried out, described below. For the most part these were conducted in conditions of steady, near laminar flow, although an attempt has also been made to gain some idea of the performance likely in waves. We consider that it is not possible to predict closely the performance of a current meter in the sea solely on the basis of its performance in the laboratory: there is no substitute for evaluation and intercomparison in situ. However, a preliminary laboratory test, made in conditions over which the investigator has some control, does allow assessment of some of the basic characteristics, and indicates those areas in which scope exists for improvement in design.

2. Measurement System

Most of the measurements have been made in the towing tank at the IOS, Wormley. The tank, filled with fresh water, is of dimensions 50 x 2 x 2 metres, and is equipped with a hydraulically driven carriage, whose speed can be preset within the range 1cm/sec - 2m/sec. Except at the lowest part of the range, speed is constant to within 1%. The tank also contains a number of windows. We have therefore been able to make some visual studies of flow past the instrument, directing liquid dye through fine capillary tubes to the required place. Both static and dynamic tests have been made. In the former the instrument is towed in a fixed attitude to the direction of motion along the tank to determine linearity and directional response. We have also tried to simulate near surface dynamic conditions by mounting on the tow carriage an apparatus which moves the instrument in a vertical circular path of adjustable diameter 25-100cm and periodicity within the range 5-33secs. This is driven by a servo-controlled motor which generally assures constancy of angular velocity to within 2%. The device also carries a shaft encoder to permit correlation of current meter output with flow incidence angle.

A block schematic of the measurement system is shown in Fig. 2(a); the orbital motion simulator is shown in Fig.2(b). In the case of the towing tests the procedure has been to take the mean of a number of measurements along the tank to allow smoothing of noisy instrument output. The logger available to us takes 10 samples/second, each sample being of 40 millisecond duration. A low pass filter was therefore included (2 stage Butterworth, cut-off 3Hz), as a precaution against aliasing although experience subsequently showed this was often not needed. The linearity of the buffer, filter and logger together was better than 0.1%.

Carriage speed is available as a variable pulse frequency analogue, obtained by interrupting a light source-detector path with a slotted wheel, geared to a ground steel wheel spring loaded on the running rail. The logger counts this continuously, sampling at 100 millisecond intervals synchronously with all other channels.

In order to permit correlation of instrumental noise with mechanical noise introduced by the carriage, or rotation device, and instrument suspension, orthogonally mounted accelerometers were strapped to the current meter. The outputs were integrated before display.

RESULTS

3. Linearity at Constant Speed

In the first series of tests the current meter was mounted in an upright position at the end of a vertical tubular spar clamped to the towing carriage and towed at constant speeds. Runs were made with each axis aligned in turn along the tank.

Alignment was made initially by eye, fine adjustment to the angular position of the spar then being made to minimize the signal from the transverse axis with the carriage moving at constant speed. The top of the spar carried a vernier scale to facilitate relative angular adjustments. The maximum towing speed (~1 metre/second) was limited by the onset of strumming of the support spar. At the other end of the scale residual circulation in the tank proved a serious handicap below a few cm/sec. The range over which we operated encompasses most speeds of practical interest, although near surface speeds may exceed 1m/sec on occasions. A more detailed study is required for very low speeds.

An unweighted linear regression has been applied to each set of data and the deviations from linearity are shown plotted against indicated carriage speed in Figs.3(a) and 4(a). The outputs from the transverse axes scaled by the appropriate calibration factor also are plotted against towing speed (Figs.3(b) and 4(b)), demonstrating that the axes were not perfectly aligned across the tank. The angle is small, however ($\sim 1^{o}$).

Later during the measurements two additional linearity checks were made: the first, shown in Figs.5(a) and (b) is directly comparable with Figs.3(a) and (b), in that the current axes were aligned along and across the tank. For the second check the spar was rotated by 45^{o} to produce approximately equal outputs from each axis at constant speed. A linear regression has

again been applied to each of these and the deviations from this fit are shown in Figs.6(a) and (b). All regressions in Figs.3-6 have included both directions of flow since this would be the method adopted by most users. However, if points for positive and negative flow directions are fitted separately the difference in slopes is insignificant and the distribution of residuals essentially unchanged, indicative of symmetry in the instrument and its mountings. The points shown in Fig.6(a) proved the one exception: fitted separately for positive and negative flow directions these showed a difference in slope of 5%, considerably greater than the standard error. We are unable to account for this individual discrepancy.

Fluctuations occurred in current sensor output at all speeds, but increasing generally with increasing speed. To indicate the degree of uncertainty in mean values thereby introduced, 95% confidence limits (assuming a normal distribution) are shown for each point plotted in Figs.3-6. The dependence of this 'noise' on speed is more clearly shown by plotting the standard deviations ($\sim$200 samples) in current meter outputs, and carriage speed, against mean speed in Fig.7. The current sensor noise always exceeds a level attributable directly to fluctuations in carriage speed, and quantization noise introduced by the sampling method is insignificant except at the lowest carriage speeds. Furthermore the levels are significantly greater for the transverse axis than for the axis aligned in the flow direction. The maximum observed in transverse axis noise at about 80cm/sec was not coincident with any noticeable maximum in vibration although there seems little doubt that the noise is of hydrodynamic origin. We discuss this further in Section 10.

To the uncertainty in determining current meter output arising from noise must be added the problems introduced by residual flows in the tank. We found that following a measurement a settling time of 15-20 minutes reduced any residual flow to a few mm/sec, but this might then persist for hours. This makes verification of linearity at low speed ($<$10cm/sec) - an important range when measuring currents at great depth in the ocean - difficult and time-consuming. Attempts were made to check for residual flow before a measurement at lower speeds by observing the displacement of a dye streak over a minute or so, but this was a rather unsatisfactory solution to a problem that needs further thought. The consequence is that we would add a further uncertainty of perhaps $\sim\pm$3mm/sec to all measurements.

Whatever the constraints on the measurements, the behaviour of the instrument in steady flows up to 1m/sec is evidently well described by a linear calibration. Departures from this are generally < 1cm/sec, although these tend to be systematic. For example, a similar distribution of residuals is found for each axis (Figs.3(a), 4(a)), and in each case this pattern has a tendency to repeat itself when flow is in the reverse direction, as shown by the anti-symmetry about the zero axis. Note also the dependence on flow direction of the cross-axis output shown by the change in slope in Fig.5(b). This is difficult to explain, although to put it into perspective it represents an angular error of $\leq 2^{\circ}$, which is within the accuracy of most compasses.

4. Azimuth response - directional response in horizontal plane with current meter mounted vertically

These measurements were made at 10° intervals at a single speed, 50cm/sec. As before, the mean of at least 200 samples was taken at each angle of incidence, and these have been combined in Fig.8 to show the vector magnitude response. The outputs for each axis as a function of incidence angle are compared individually with the ideal sine and cosine functions in Fig.9. An indication of the way in which the noise level varies with flow incidence angle is given in Fig.10.

The sensitivity is little affected by change in angle when flow is incident within $\pm 20^{\circ}$ of an axis; this coincides, also, with minimum noise ($\sigma \sim 0.4$cm/sec). Between 20° and 30° the output reduces by 10%, accompanied by an increase in noise level ($\sigma \sim 1.0$cm/sec). Further increases in azimuth produce a gradual improvement in sensitivity, shown by the comparison with sine and cosine curves in Fig.9, and a reduction in noise level (Fig.10). Note also in Fig.10 that when an axis is aligned with the flow, the noise introduced directly by carriage vibration accounts for about half the observed total (σ = 0.4cm/sec) in current meter output. However the noise level in the transverse output is significantly higher ($\sigma \sim$ 0.7cm/sec).

We believe that these departures from uniform response in azimuth are largely attributable to the effects of the wakes from the reflector support cage. Thus a near constant sensitivity and a low noise level are obtained from the longitudinal axis until it is rotated sufficiently far to intersect a wake. This region contributes lower mean velocity and disturbed (though at this distance not turbulent) flow. The much greater noise level obtained from a transversely directed axis arises because the sound path intersects two wakes.

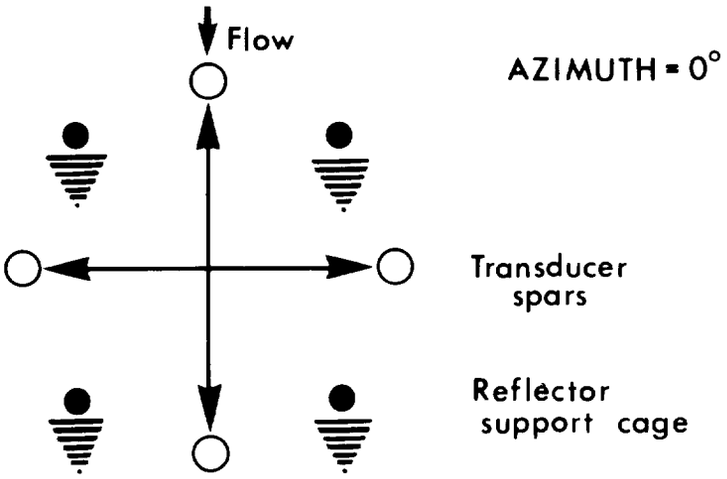

SCHLICHTING (1955) has derived expressions permitting the calculation of mean flow at points in the wake behind a cylinder. These are strictly valid only for rather greater distances than those present here, but they enable estimates to be made of the reduction in mean flow, to within perhaps 25%. Using these expressions and knowing the geometry of the system, we have deduced the mean velocity profile along the sound path between transducers for the case when azimuth angle = 45°. This supposes that any flow disturbances near the transducers or reflector are small.

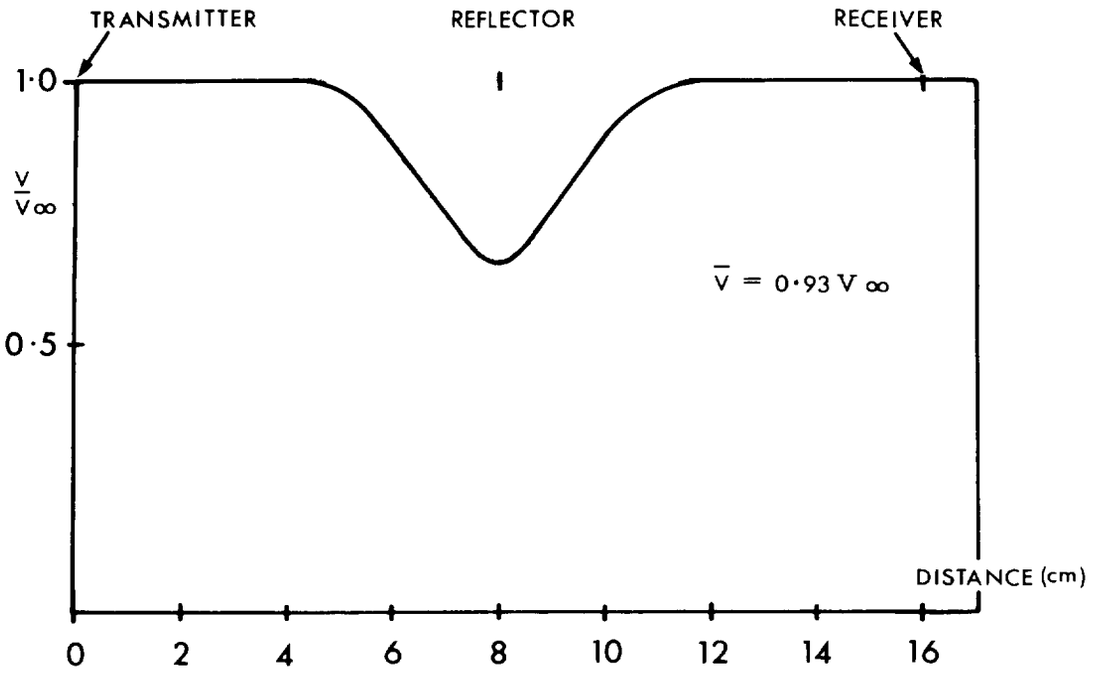

Approximate profile of fluid velocity, calculated as a fraction of free stream velocity V_{∞}, along acoustic path between transducers for azimuth = 45°

On integrating this profile we find that the velocity measured by the instrument should be $\sim 0.93\ V_\infty$, giving good agreement with observation (Figs.8,9).

Although these measurements were conducted at 50cm/sec the scaling within the wakes should not alter significantly with speed. We should therefore expect to find a similar response to Fig.8 at other speeds. This is confirmed by the linearity of output with speed, accompanied by 7% difference in sensitivity, found for calibrations at $\theta = 0$ and 45° (Section 3).

5. Tilt Response

A series of measurements were made with the instrument inclined slightly from the vertical. In practice the current meter support in a mooring would contain a form of gimbal to maintain the instrument in a vertical position. Nevertheless it is desirable to know the extent to which the cosine response is obtained in the vertical plane, in the absence of any such arrangement. Measurements were made at steady speeds of 6, 12, 24, 36 and 72 cm/sec, for tilt angles (ϕ) of 0°, 10°, 20°, 30°. These were set using a hand held inclinometer, and the setting accuracy is estimated to be $\sim \pm 2^\circ$. Two sets of runs were made, firstly with the azimuth angle, θ nominally zero: one axis was aligned along the tank but tilted through angle ϕ and should therefore record $V \cos \phi$. The remaining axis was directed transversely and should give ideally zero output.

The results for the longitudinal axis, normalised to the output at $\phi = 0^\circ$, are plotted against ϕ in Figs.11(a)-(d). Note that the vertical error bars denote the standard deviations of all samples from the mean, expressed as a fraction of the output, and, thus related, the noise appears to decrease with increasing flow, at any given angle, although in absolute terms the noise actually increases slowly in the manner shown in Fig.7. Tilting the instrument clearly affects the noise, which generally increases with angle, and which also is rather greater when the lower part of the instrument is directed into the flow. Progressive obstruction of the flow by the leading transducer spar suggests itself as the most likely cause. Fig.11 shows that when one axis is aligned in the flow direction, increasing tilt causes the output to fall off slightly faster than the ideal cosine response: for angles within $\pm 20^\circ$ of the vertical the difference is less than 5% and at the lowest speeds (6 and 12cm/sec), the ideal response is followed very closely.

We also looked briefly at the more general case when flow is incident between the axes. The current meter was rotated through 45^{o} (nominal) in its vertical position (azimuth angle $\theta = 45^{o}$) prior to tilting. The transducers were thus disposed symmetrically about the flow direction. The results are again normalised to $V_{\phi=0}$, and are plotted in Figs.12(a)-(d). Note that as in Fig.11 error bars denote standard deviations for V_{ϕ} only: calculation of the standard error for each mean should also include the standard deviation for $V_{\phi=0}$, which is of the same order. The noise levels in Figs.12(a)-(d) are noticeably greater than in Figs.11(a)-(d), presumably because the wakes from the reflector support struts now intersect the acoustic paths, as discussed in Section 3. There is also a significant scatter of the means, particularly at the lower speeds. We do not know the cause of this, unless residual flows were particularly strong during these runs. Generally these were estimated to be within ±3mm/sec, which in Fig.12(a) represents ±0.05 in $V_{\phi}/V_{\phi=0}$. The overall impression from the data is that the response falls off only slightly faster with angle of inclination than the ideal cosine response. As before the noise increases markedly when the transducers are tilted away from the flow, but, in contrast to the previous findings, (Fig.11), reduces slightly for progressive inclination into the flow.

A series of runs were also included for tilt angles approaching 90^{o} These were made primarily to confirm some results discussed in Section 8 and they show clearly the effect of the reflector wake* when flow is nearly coaxial with the instrument case. Since the current meter was necessarily mounted horizontally for the tests, the inclination angles are from the horizontal position. (Fig.13).

6. Current meter stability and temperature coefficient

A check was made for any gross variations of current meter output with temperature change by immersing the instrument directly in a stirred water bath whose temperature could be preset between 2^{o} and 22^{o}C. Measurements were made at 8 temperatures; on attaining each temperature the stirrers were switched off and the system allowed to settle for a minimum period of an hour, relying on tank insulation to maintain the temperature below ambient. A series of readings were then made and the mean taken. The procedure was later repeated twice, increasing and decreasing the temperature within the range 6^{o} - 20^{o}C.

---

* The version of the instrument intended for profiling applications has parallel transducer spars, and direct acoustic paths: a reflector is not used.

The measurement showed no particular pattern or trend. At all temperatures the output from the instrument amounted to a few tens of millivolts. Within any one series of readings the standard deviation about the mean was very small, typically 0.5mV or 0.1mm/sec in flow. For series which had been repeated, with several temperature changes in between, reproducibility of the means was only to within a few mm/sec. Throughout the temperature range 2^{o}- 22^{o}C all readings lay within a spread of 60mV or 1.5cm/sec. The cause of this scatter is not known; although checks on the measurement procedure enable residual flows to be ignored as insignificant. Temperature gradients of less than 0.5^{o}C developed in the tank within an hour of switching off the stirrers, but the consequent changes in sound velocity are insufficiently large to account for the observed scatter.

7. Stability

The stability of the instrument was checked over a two week period at a constant temperature (18.0^{o}C). As before, stirrers were switched off approximately one hour before each series of 30 readings, and residual flows in the tank could be safely neglected. Results are plotted in Fig.14, whence it can be seen that scatter on the series means, $\leq$ 1mm/sec, is considerably less than that obtained for similar measurements following changes in temperature. During the 300 hour period of the measurements there is clearly a gradual change in the output of both axes, of $\sim$ 5mm/sec. This is of the same order as changes in zero noted in the towing tank tests over a period of weeks, and it is representative of the stability of this particular instrument.

8. Dynamic Tests

One of the more difficult measurements to make in the sea is that of mean near-surface current. For some scientific purposes the aim is to achieve an accuracy approaching 1cm/sec. In the presence of wave orbital velocities which can exceed 1m/sec, this requires a very high degree of linearity and uniformity of directional response. Although this form of the acoustic meter has not been expressly designed for work in the near surface region, we wished to know to what extent it might prove suitable in waves.

In some earlier testing of electromagnetic sensor heads (GRIFFITHS and COLLAR, 1977) we had attempted to simulate the accelerated flow of waves by moving the sensor at constant angular speed in a vertical, circular path

in the towing tank. Whilst this does not reproduce wave conditions exactly, it nevertheless offers a useful test and so we attempted to apply it to the acoustic meter. Some practical problems were encountered in that the apparatus had been constructed to meet the much lower weight and drag requirements of electromagnetic sensor heads. As a result the acoustic instrument was subjected to rather more vibration than anticipated, but we do not think that this invalidates the results.

A series of measurements were made at periods between about 6 and 25 seconds with the towing carriage stationary. Representative sets of results are shown in Figs.15, 16 and 17, traced directly from the analogue recorder output. These include the outputs from both current meter axes, the integrated output from the accelerometer, and the shaft encoder output, which has enabled identification in each figure of the instantaneous direction of flow. Broken lines indicate the ideal cosine response for the current sensor: encircled points (cosine function) in Fig.17 show that the angular velocity of rotation was nearly constant. Note that the phase of the accelerometer output, mounted in each case coaxially with Axis 1, differs appreciably from the current meter output. This shift is produced by the integrator, which has a high-pass response cutting off (-3dB) at 0.3Hz. Any mechanically induced noise present in the current meter record above this frequency should thus correlate fairly well with the accelerometer output. The correlation is good, for example, when the system is started from rest (Fig.16). This causes a transient oscillation of the spar at a frequency of $\sim$2.5Hz, which decays within two or three seconds, and which is clearly visible in current meter and accelerometer traces. The oscillation is present, also, in Fig.17, although on this occasion it persisted rather longer. At times mechanical vibration was noticeable, though at a relatively low level, throughout the cycle (Fig.15). However, quite apart from mechanical imperfections, which in this relatively simple arrangement we have found difficult to eradicate, there are uncorrelated departures from the ideal current meter response. These occur at a similar point in each successive cycle, although the exact form of the trace differs slightly from cycle to cycle. Apart from the transient oscillation, the first cycle does not differ appreciably from succeeding cycles. These departures from the ideal response result from flow obstruction by the instrument itself. By reference to the output from the shaft encoder three sources of hydrodynamic noise can be identified:

(a) The reflector wake when the instrument is moving vertically downwards through the water. This is noticeable in each of the Figs.15-17 for axis 1; but in each case there appears to be little noise generated in axis 2. Note that the form of the sensor response appears similar to that obtained over a limited angular range in the static tests (Fig.13).

(b) Obstruction of the flow by the instrument housing. In view of dimensions of this particular instrument in relation to the orbital diameter (50cm) this not unexpectedly affects the outputs from both axes, (Figs.15, 16). A substantial reduction should be achieved by mounting the transducers further from the housing.

(c) Stagnation of flow near the transducer faces. This may occur when the flow is incident on the spar behind the transducer face, but it takes place concurrently with flow obstruction by the housing and is therefore difficult to distinguish. For some measurements we reduced the orbital diameter to 25cm, at which the modification of the flow by the housing should be greatly reduced. The trace (Fig.17) does change by comparison with Fig.15, 16 and this may indicate that the transducer wake is assuming a relatively greater importance.

9. Observations using dye

We attempted to confirm the existence of wake effects by making visual observations. A series of fine capillary tubes were so arranged that a dye solution could be discharged continuously at selected points in the acoustic path. By recording the sequences on film it was hoped that a measure of the perturbation of the flow might be made for comparison with the current meter output. A comparison in this detail has proved impractical, but the dye observations have strongly supported, albeit in a qualitative sense, the conclusions outlined above.

10. Noise

Reference has been made in earlier sections to the rapid fluctuations in current meter output in steady flow conditions, and the way in which their amplitude varied with instrument orientation and speed of flow. It has been shown that they arise mainly from flow obstruction by identifiable parts of the instrument. For many purposes these fluctuations in output are relatively unimportant, because they occupy a different part of the frequency spectrum to the variables under observation. Sampling and averaging times can therefore be chosen to smooth the output without risk

of aliasing. However it was not clear whether the level or spectral distribution of the noise were much affected by the method of supporting the instrument. Some experiments were made to determine this.

A series of runs at constant speeds (35, 60 and 100 cm/sec) were made along the tank with the instrument mounted vertically beneath a 5cm diameter tubular spar, of circular cross-section, clamped to the towing carriage. The current meter axes were directed along and across the tank, and accelerometers were strapped to the housing, similarly aligned. The outputs from the accelerometer integrators and current meter, short records of which are shown in Fig.18, were sampled on line by a Data General NOVA computer, which carried out a spectral analysis on each record using an FFT sub-routine. Our choice of sampling frequency, 62.5Hz was governed partly by the equipment available to us (not intended specifically for this application) and partly by the wish to examine the full 10Hz bandwidth of the current meter: the length of record available at maximum speed ($\sim$20 seconds) limited the low frequency resolution. Prior to sampling all outputs were bandpass filtered (two stage, cut-off frequencies 0.1, 25Hz) to ensure freedom from aliasing and to remove the large d.c. offset present on some signals.

Some representative spectra are shown in Fig.19(a)-(d). Repeated runs at the same speed showed analyses of the integrated outputs from the accelerometers to be reproducible. At each of the three speeds the principal vibration mode across the tank took place at a constant frequency equal to the natural frequency in still water (4Hz). Along the tank the spectral distribution of oscillations was rather broader, but dominant frequencies were still readily identifiable. These were noticeably speed dependent: $\sim$1.0Hz at 36cm/sec, 1.8Hz at 60cm/sec and 3.0Hz at 1 metre/sec. A broader distribution might be expected in this case, since vibration introduced by irregularities in carriage speed would occur along, rather than across, the tank. This may account for the subsidiary peak below 1Hz evident in Fig.19(a). The main energy is thought to arise from another cause, however. The forces acting on a cylindrical spar in steady flow are related to the shedding of vortices: the frequency of shedding, f_v, the flow rate, V, and the cylinder diameter, d, are related over a wide range of Reynolds numbers by the dimensionless Strouhal constant $S \sim f_v d/v \sim 0.2$. Normal to the plane of the flow the frequency of the force is that of the vortex shedding: in the plane of the flow it is at twice this rate. In the present case ($d \sim 15$cm, f is thus $\sim$ 0.48 at 36cm/sec, 0.80 at 60cm/sec and 1.33 at 100cm/sec), corresponding fairly closely to values obtained in practice. In the

direction of flow the current meter mounting is therefore apparently driven at a rate determined by vortex shedding from the instrument casing, rather than at the natural frequency of the spar,which seems to be largely damped out.

The spectral distribution of the currents differed appreciably from the vibration spectra: they were not reproducible for runs at similar speeds and the main vibration frequencies determined from the accelerometer records were not readily identifiable. Speed did not greatly affect the distribution: the most energetic fluctuations were invariably found below 1 or 2Hz. Comparison of the spectral envelopes in Fig.19(c), (d) shows also that the cross axis noise occupied a much wider band than noise generated in the longitudinal path.

We then analyzed some records obtained from the current meter when mounted beneath a streamlined spar, approximately 8.5 x 4.0cm in section with 0.5cm wall thickness. (The inclination response measurements were made using this spar.) Records at two speeds, 30 and 70cm/sec, were digitized at a 20Hz rate from u/v recorder records before analysis by FFT. A typical analogue record of the current sensor output at 35cm/sec with axes are aligned along and across the tank is shown, together with the transverse velocity obtained from an accelerometer, in Fig.20. It should be compared with Fig.18,obtained using the circular spar at 45cm/sec. A comparison of r.m.s. noise levels at similar speeds using the two types of spar shows no significant differences.

The spectral analyses of data obtained with the streamlined spar largely agree with the previous findings: this spar has natural vibration modes in still water of 7Hz along the tank, 4.7Hz across the tank. The 4.7Hz mode accounted for almost all the transverse vibrational energy at both 30 and 70cm/sec carriage speed. The longitudinal spectrum at 30cm/sec has peaks at 7Hz, 6.6 and 1.0Hz, while at 70cm/sec the 7Hz peak has disappeared completely and the major contribution is at 2.1Hz. The frequencies 1.0 and 2.1Hz are again sufficiently close to $2f_v$ to suggest that at 70cm/sec the behaviour of the spar in the longitudinal direction may again be dominated by vortex shedding from the instrument case; although at 30cm/sec this mode appears to co-exist with the natural mode of the spar. The spectral distributions of the currents are again considerably broader than the corresponding accelerometer data would imply, with maximum energy lying between 0.5 and 2Hz, a greater spectral width again occurs for the transverse axis.

From the limited number of measurements made we conclude that the method of mounting the sensor has little effect on noise levels or spectral distribution. It is surprising that maximum energies in the noise spectrum should occur at much lower frequencies (0.5 - 2Hz) than the dimensions of the obstructions to flow would suggest: the reflector support strut is of ~ 1cm diameter and should shed vortices at ~ 7Hz at 35cm/sec, for example. Also there seems to be no counterpart in the current records to the most energetic vibrations of the mounting spar. We have been careful to eliminate tank turbulence as a cause of noise by leaving the tank for 48 hours between runs: also by following higher speed runs with low speed measurements and vice versa for comparison. In neither situation was residual turbulence found to have a significant effect on the measurement. Since these measurements were made some similar work has been done on electromagnetic current meters, using three types of sensor head: discus, toroidal and spherical. Two of these show a similar spectral distribution of the noise, although the magnitudes are consistently lower relative to the mean speed.

11. Conclusions

The measurements described in this report do not represent an exhaustive assessment of the instrument. Many have been made with possible near-surface applications in mind, and relatively fewer have been made, for example, at the low flow rates encountered typically at great depth in the ocean. This is an area for which the instrument, with its very high resolution in flow, is particularly well suited. However the measurements should provide some indications of performance in this area also, even if incomplete.

It is difficult to summarize adequately the overall performance of the instrument, since much depends on the way in which it is to be used, and for what purpose. It is clear, however, that in linearity, resolution and speed of response the sensor represents a distinct advance over the 'first generation' rotor and vane current meters presently in use. The main limitation to making an ideal measurement now seems to be obstruction of the flow by the instrument itself, although the stability of the instrument with time may be marginal for some applications. From purely hydrodynamic considerations, improvements could be made by mounting the transducer assembly further from the housing, by redesigning the reflector

supporting cage and by reducing the diameter of the reflector itself.*

Finally, we have become increasingly conscious during these measurements that development of the present (and other) second generation instruments, with greater flow resolution and shorter response times than earlier rotor and vane types, requires greater precision in testing and calibration methods than necessary hitherto. The evaluation of sensor performance at low flow rates (<10cm/sec) is a particular area in which we have encountered difficulty and to which further attention needs to be given.

Acknowledgements

We are grateful to the Christian Michelsen Institute for the loan of the acoustic current meter. We gladly acknowledge also the help of our colleagues: J.J. Langford, G. Griffiths and C. Woodley.

References

GRIFFITHS, G, P.G. COLLAR and A.C. BRAITHWAITE. The characteristics of electromagnetic current sensors in laminar flow conditions. IOS Report No. 56 (In preparation) 1977.

GYTRE, T. The use of a high sensitivity ultrasonic current meter in an oceanographic data acquisition system. The Radio and Electronic Engineer. Vol.46, No.12, pp.617-623, 1976.

SCHLICHTING, H. Boundary Layer Theory. pp.492-496. English Ed. 1955, published by Pergamon Press Limited, London.

---

* Since this report was first written the instrument has been modified internally to improve stability and reduce temperature effects. Also, the reflector support struts, and the reflector itself, have been reduced in diameter. This should result in a significant improvement in the sensor performance.

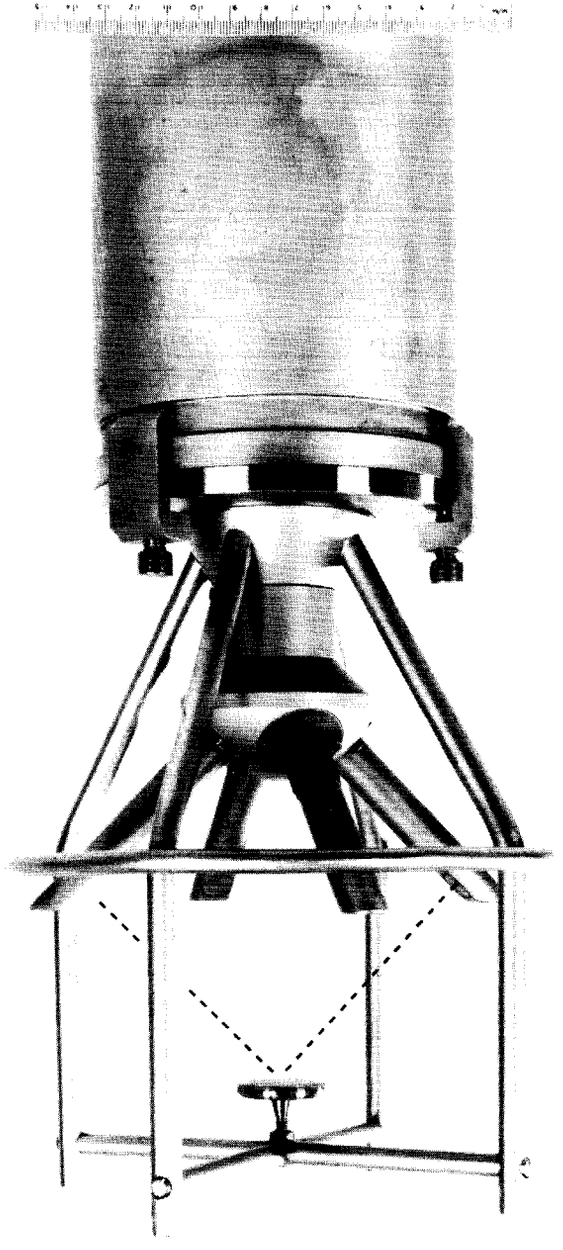

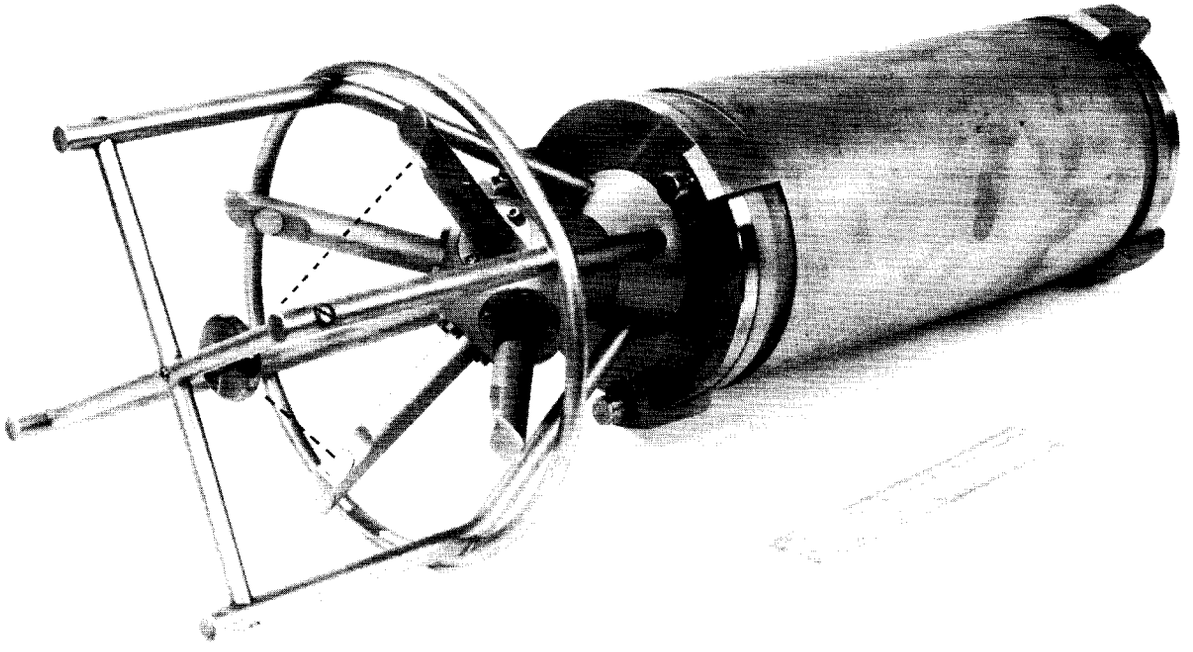

Fig. 1 General view of current sensor.
(Acoustic path via reflector shown for one axis by broken line)

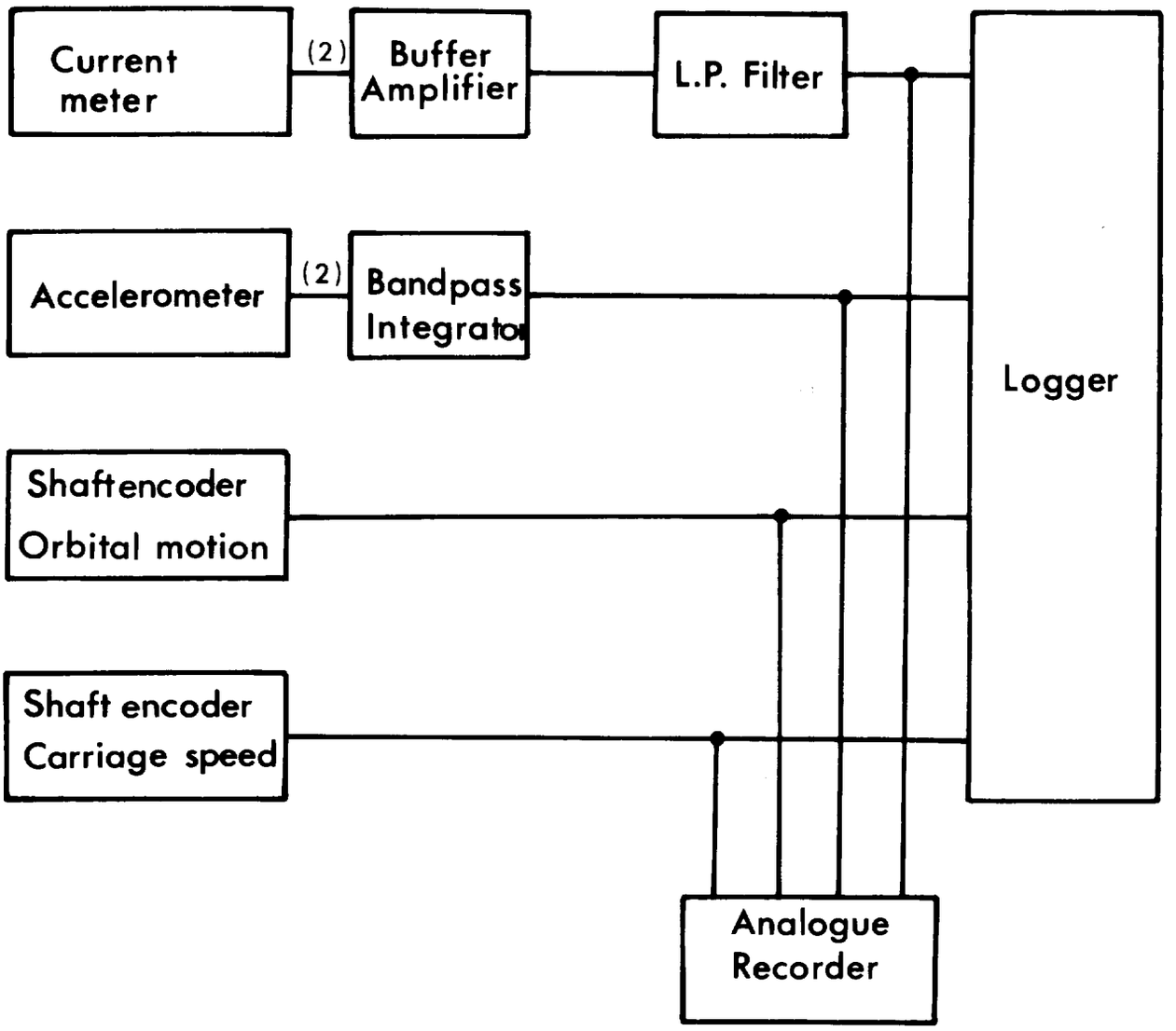

Fig.2(a) Block schematic of measurement system.

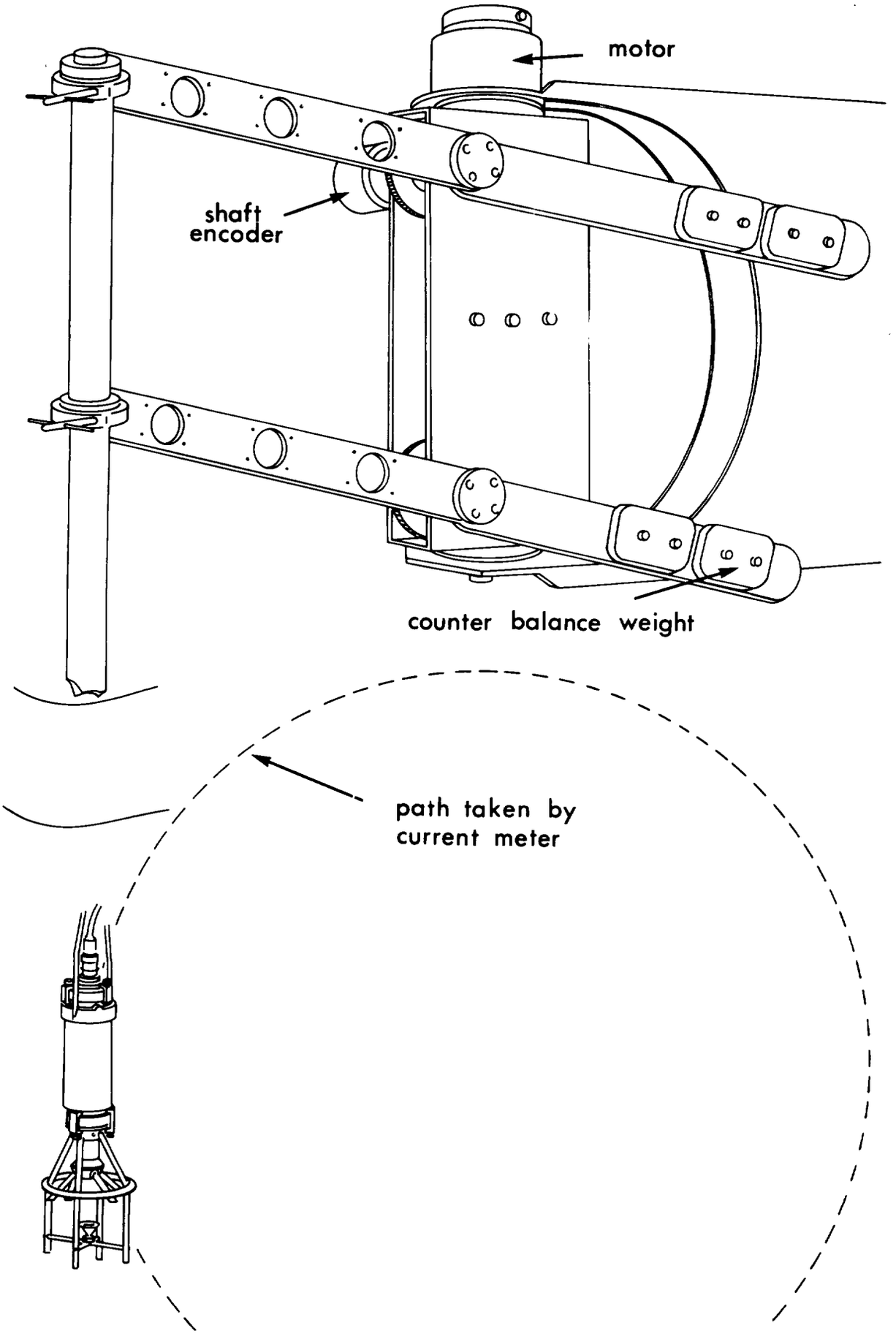

2(b) Orbital motion simulator.

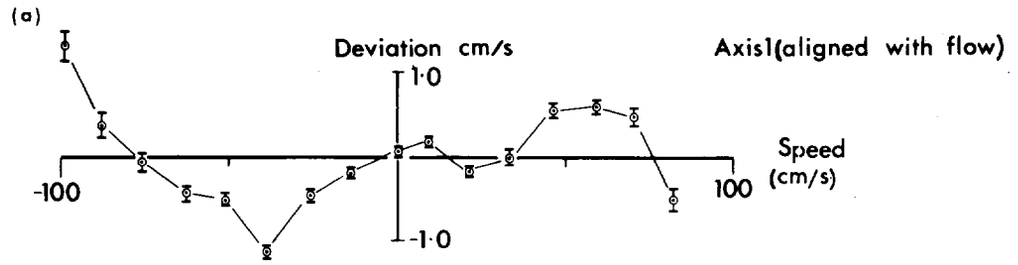

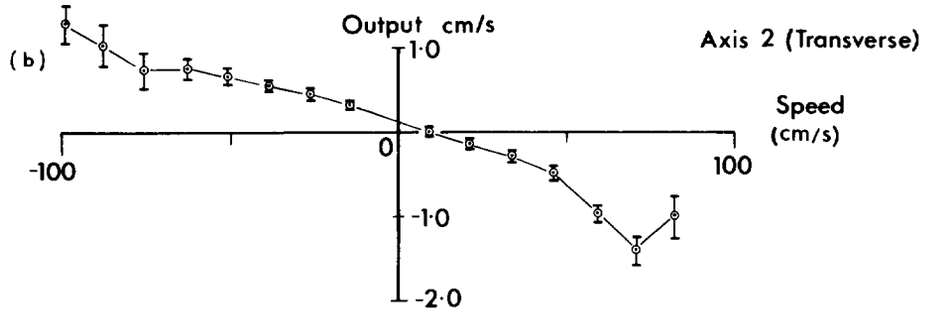

Fig.3(a) Deviation from linearity plotted against towing speed - Axis 1 in flow direction.

3(b) Axis 2 output - aligned across tank.

Note: Error bars denote 95% confidence limits (200 samples). Ordinate has been multiplied by fitted calibration factor to give cm/s units.

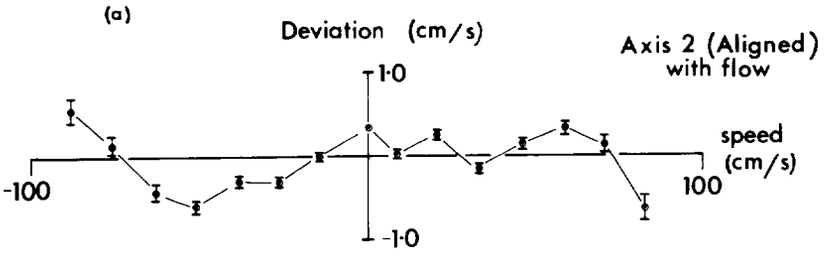

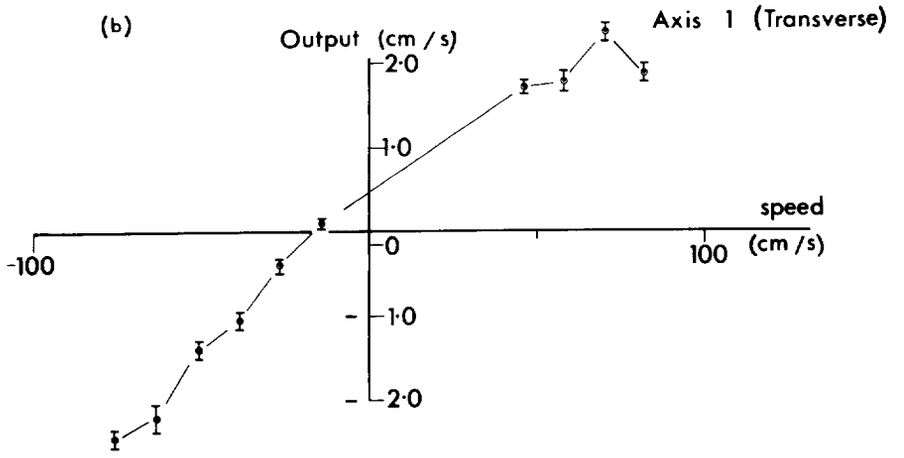

Fig.4(a) Deviation from linearity plotted against towing speed - Axis 2 in flow direction.

4(b) Axis 1 output - aligned across tank.

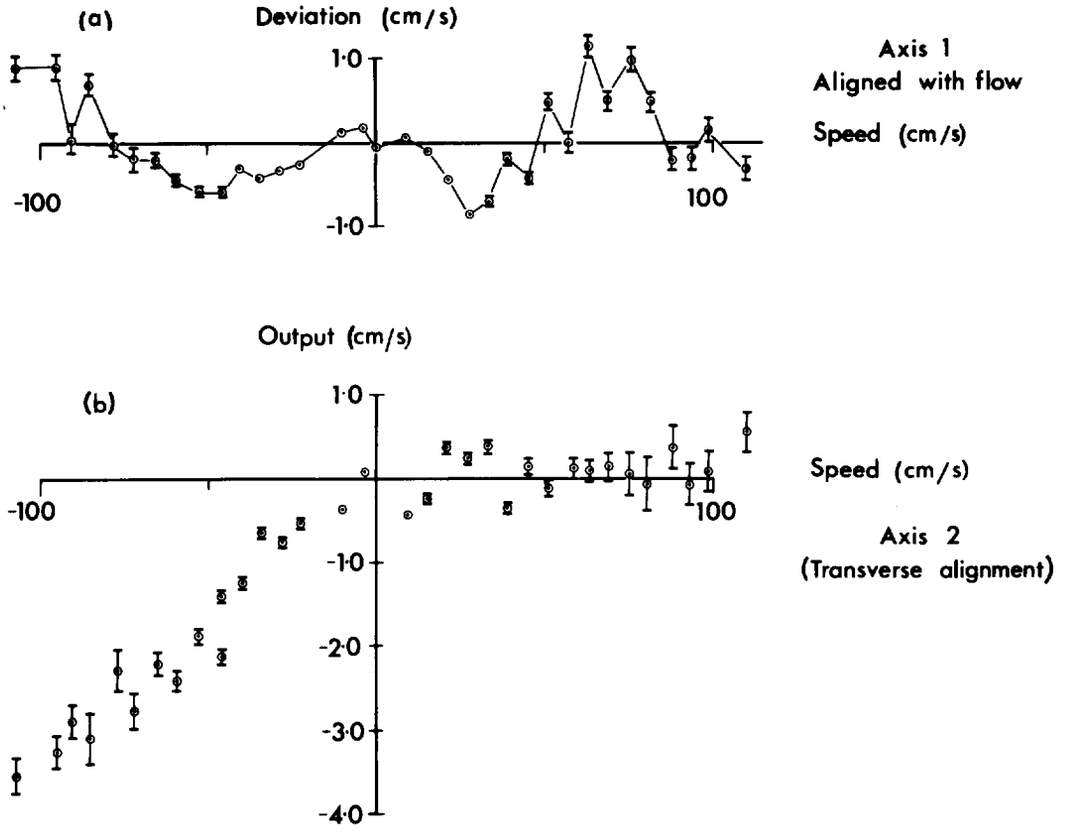

Fig.5(a) Deviation from linearity plotted against towing speed - - Axis 1 in flow direction.

5(b) Axis 2 output - aligned across tank.

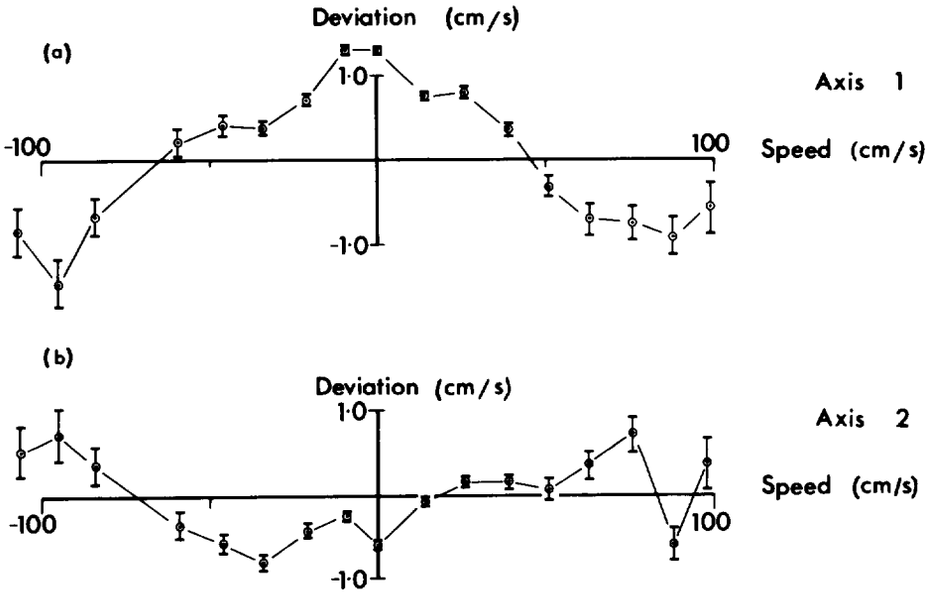

Fig.6 Deviation from linearity plotted against towing speed. Both axes aligned at 45° to flow direction.

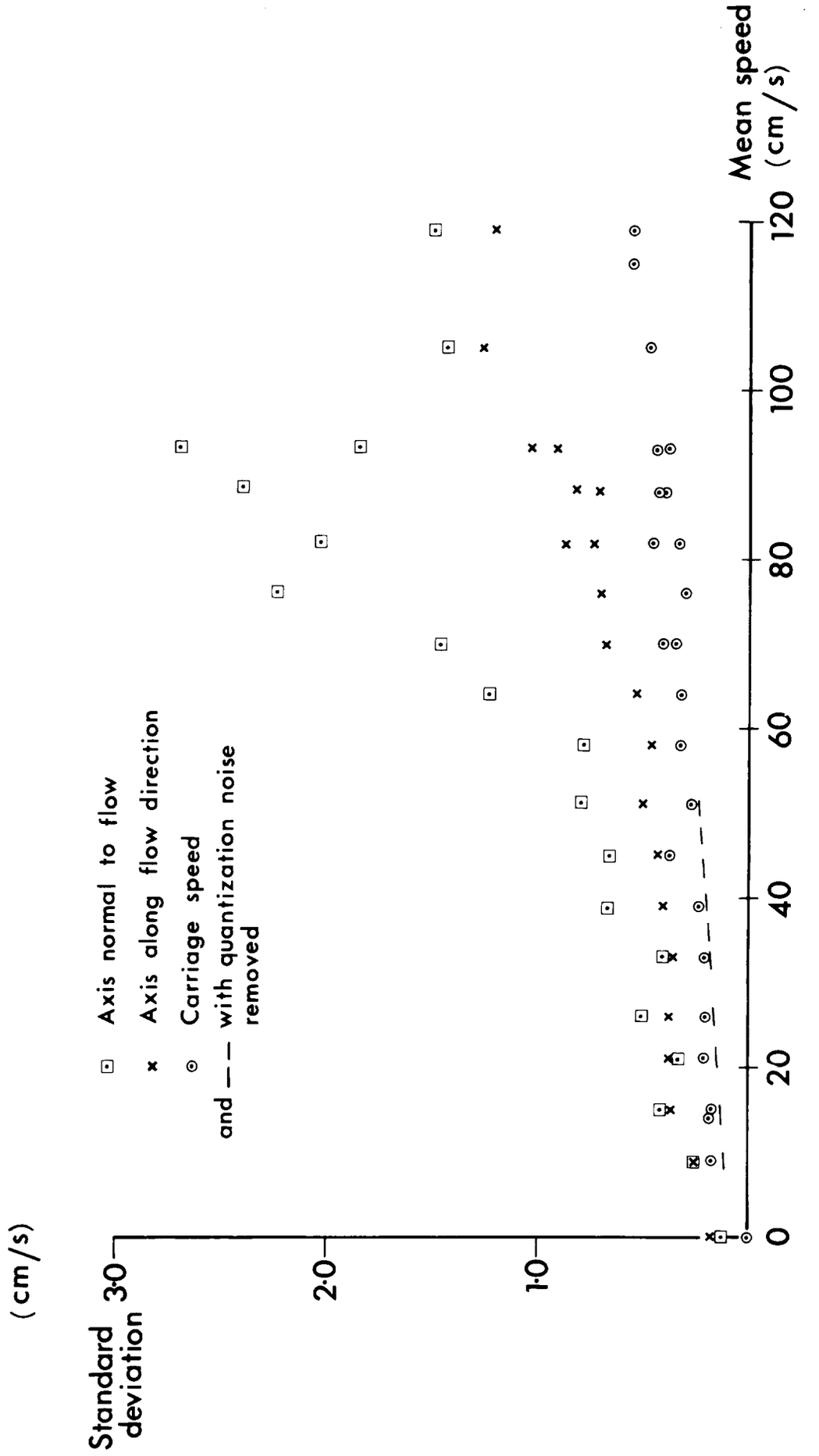

Fig.7 Variation of standard deviation of current sensor output with mean speed of tow. (Instrument mounted vertically)

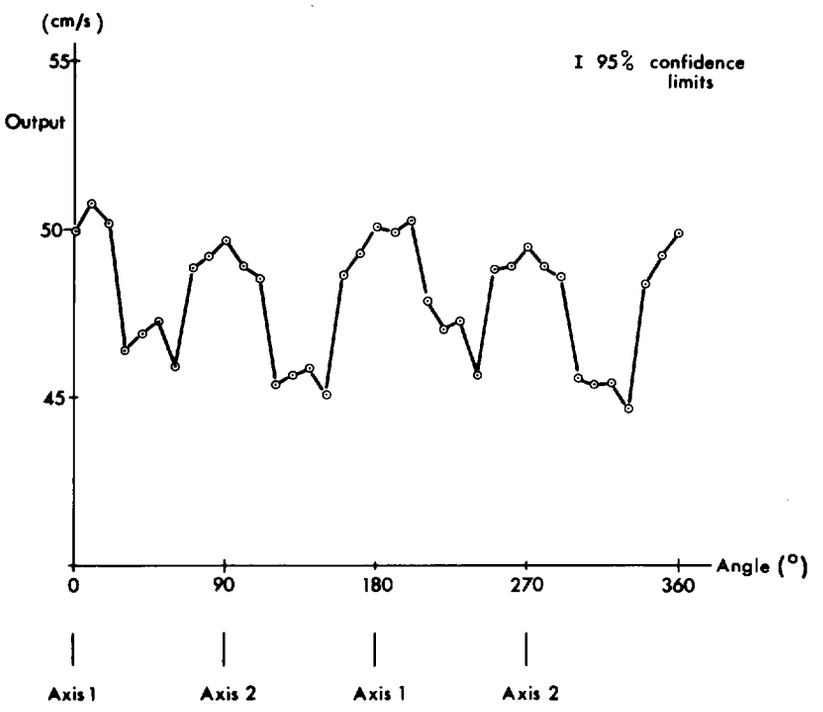

Fig.8 Response of vertically mounted current sensor to steady flow in horizontal plane at 50cm/s. Modulus of vector resultant of Axes 1 and 2 outputs.
(Axis 1 in line with flow at 0^{o}, 180^{o}
Axis 2 in line with flow at 90^{o}, 270^{o})

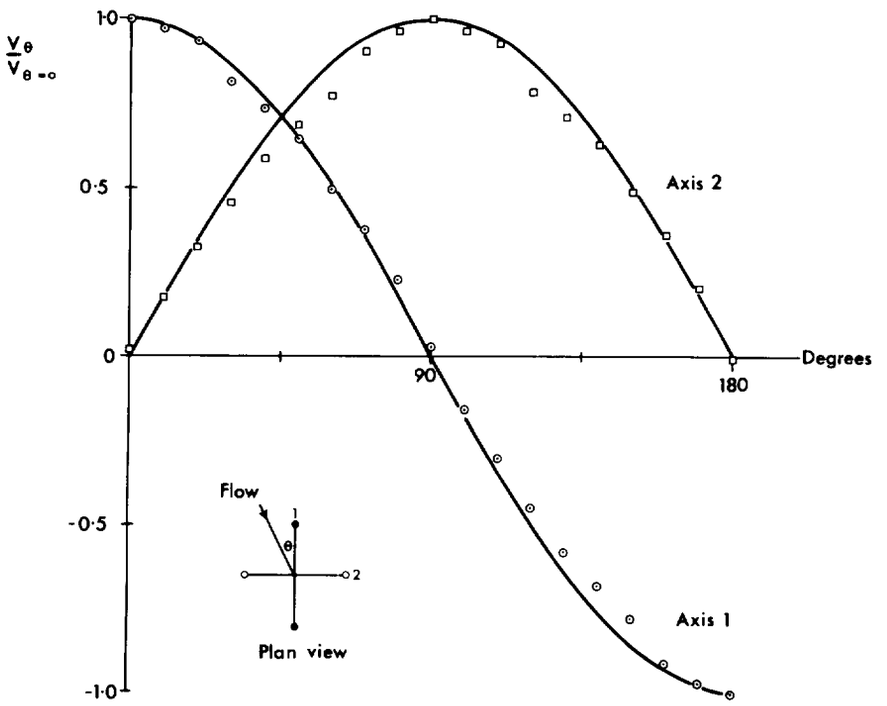

Fig.9 Outputs of axes 1 and 2 plotted individually as functions of flow incidence angle in horizontal plane - azimuth response. Speed = 50cm/s.

Note: Solid curves are sine, cosine functions.
95% confidence levels are generally of same order as size of plotted symbol.

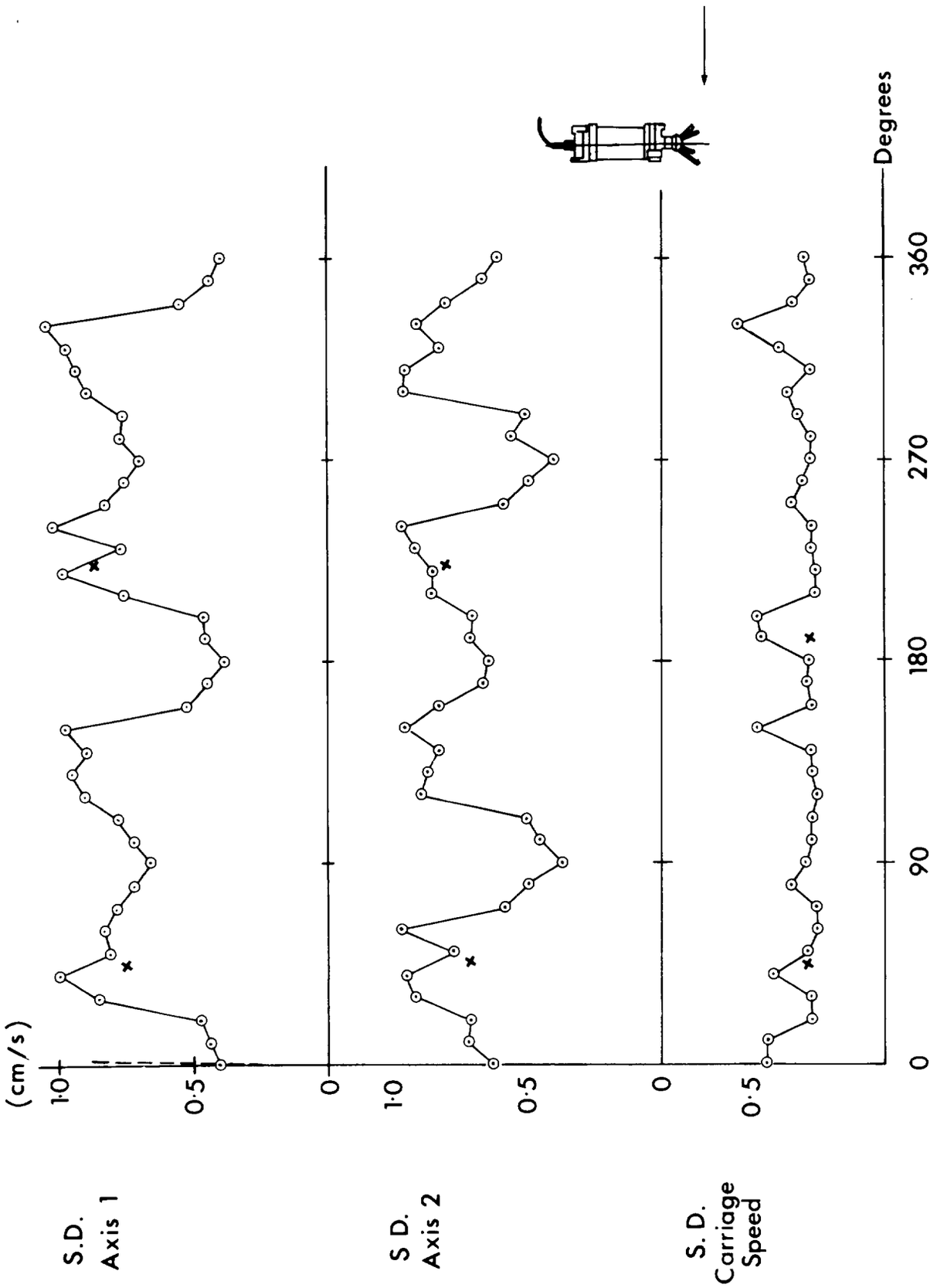

Fig.10 Standard deviations from mean outputs (Fig.9) plotted against horizontal azimuth angle.

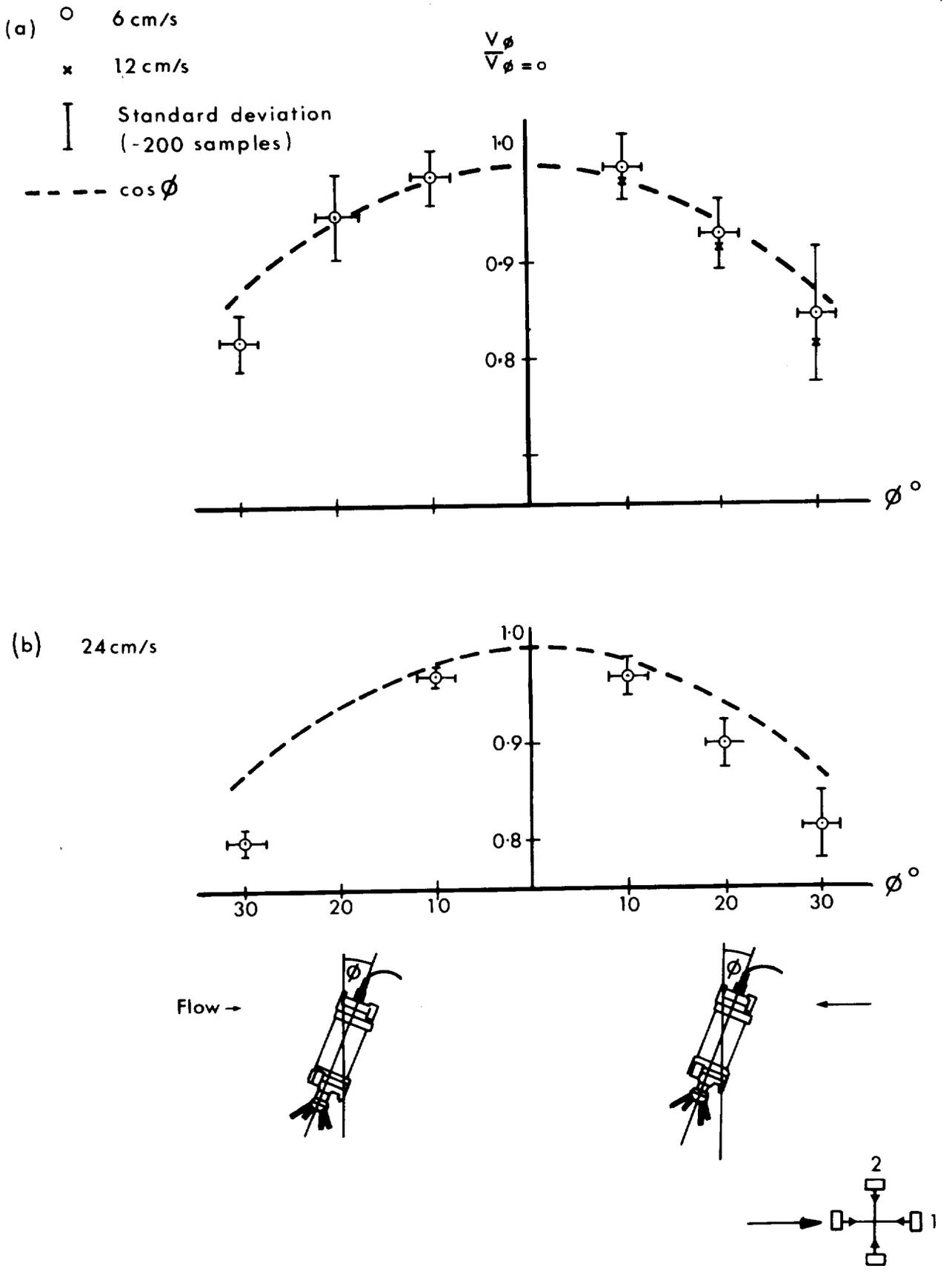

Fig.11 Response of towed current sensor tilted from vertical at a fixed angle, ϕ. Azimuth $\theta = 0^{\circ}$

Note: Error bars denote standard deviations, τ, for V_{ϕ} only. For τ shown as ± 0.05, 95% confidence interval on the mean $V_{\phi}/V_{\phi=0}$ is typically ± 0.01. In addition the uncertainty in residual flow contributes possibly ± 0.05 at 6cm/s but < 0.01 at 70cm/s.

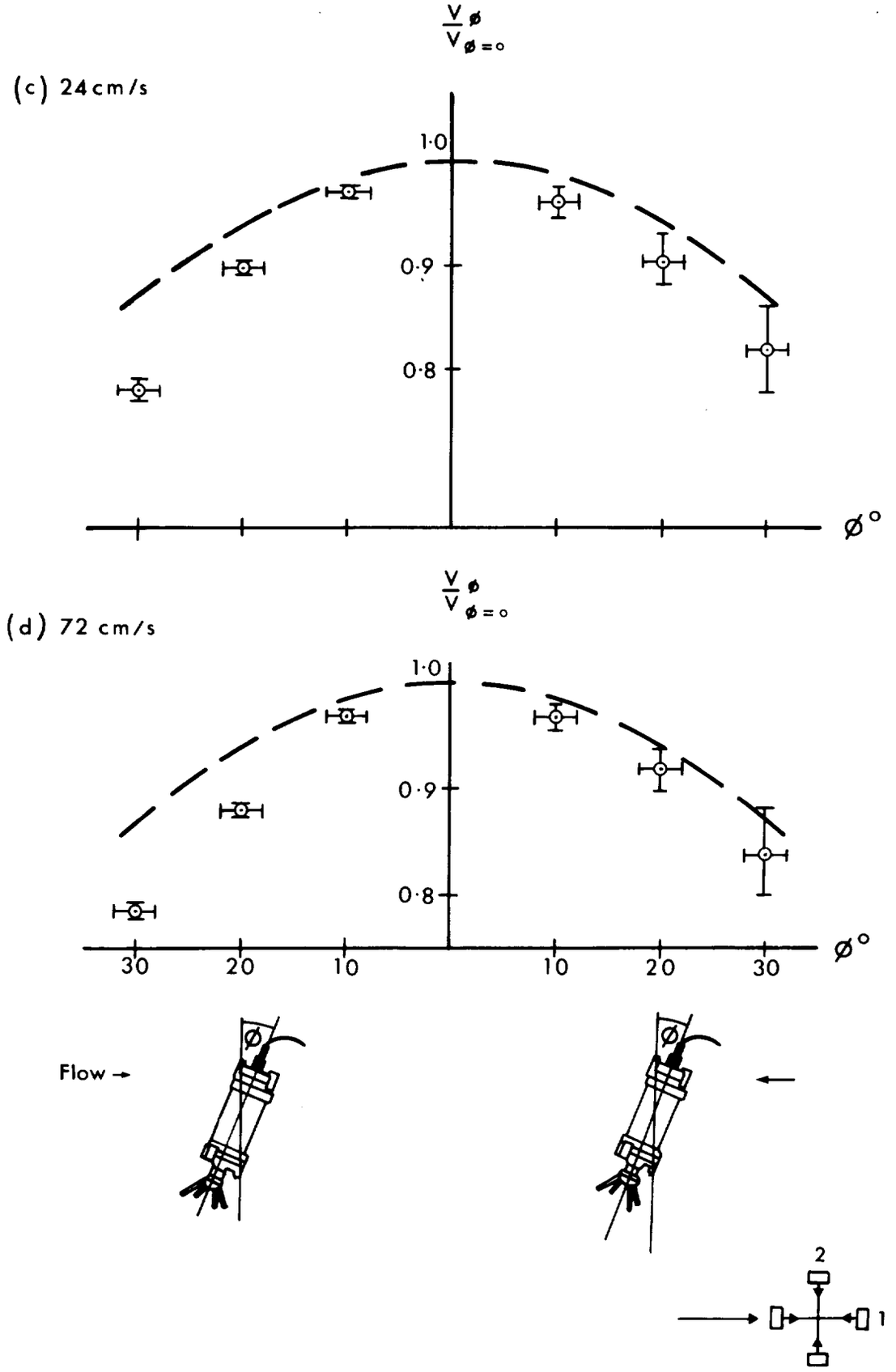
(c) 24 cm/s
V_ø / V_ø=o
1·0
0·9
0·8
ø°
(d) 72 cm/s
V_ø / V_ø=o
1·0
0·9
0·8
30
20
10
10
20
30
ø°
Flow →
2
1

Fig.11

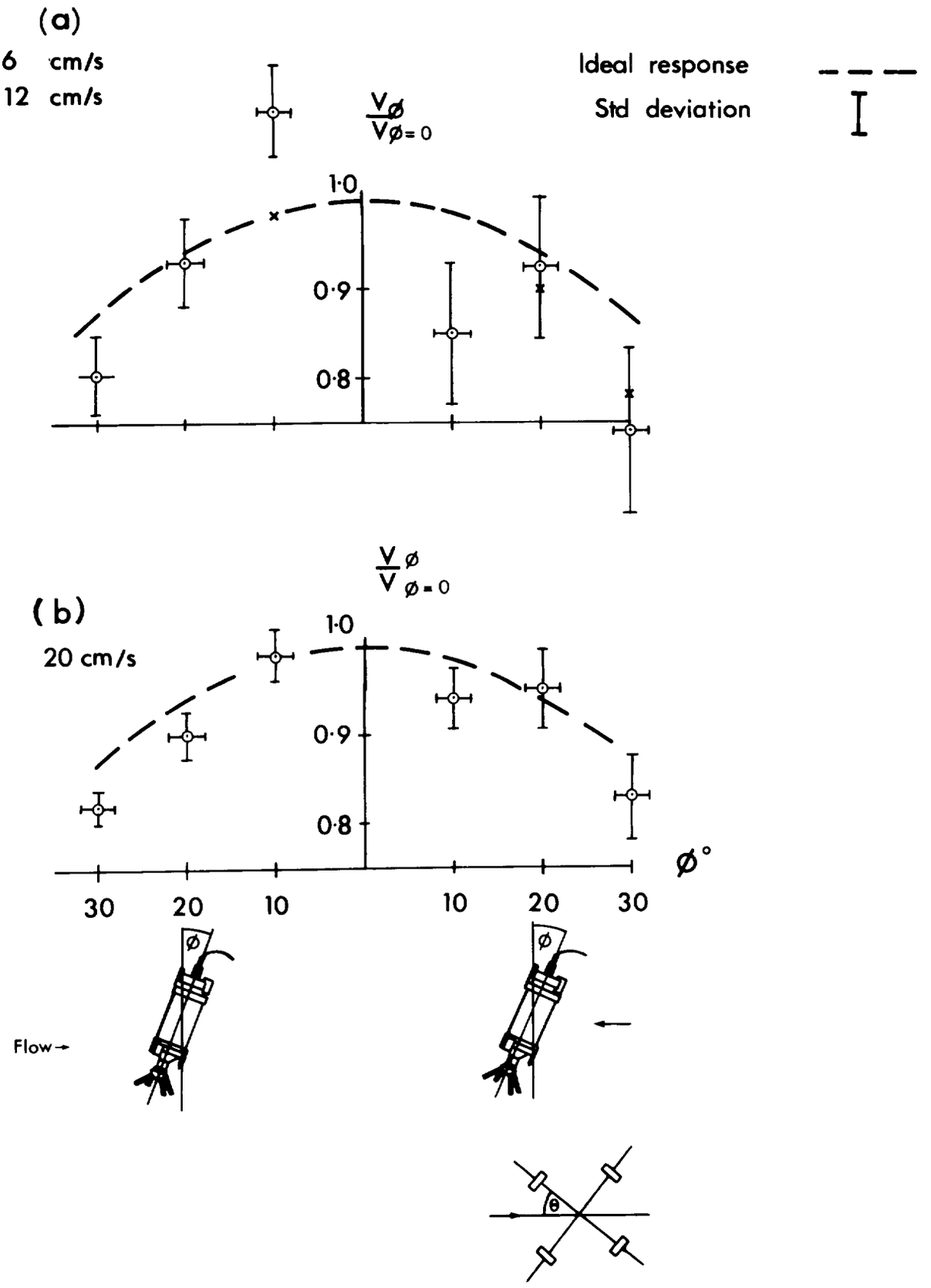

Fig.12 Response of towed current sensor tilted from vertical at fixed angle ϕ. Azimuth $\theta = 45^{o}$.

Note: Error bars denote standard deviations, σ, for V_{ϕ} only.

For σ shown as ± 0.05, 95% confidence interval on the mean $V_{\phi}/V_{\phi=0}$ is typically ± 0.02. In addition the uncertainty in residual flow contributes possibly ± 0.05 at 6cm/s but < 0.01 at 70cm/s.

(c) 36cm/s

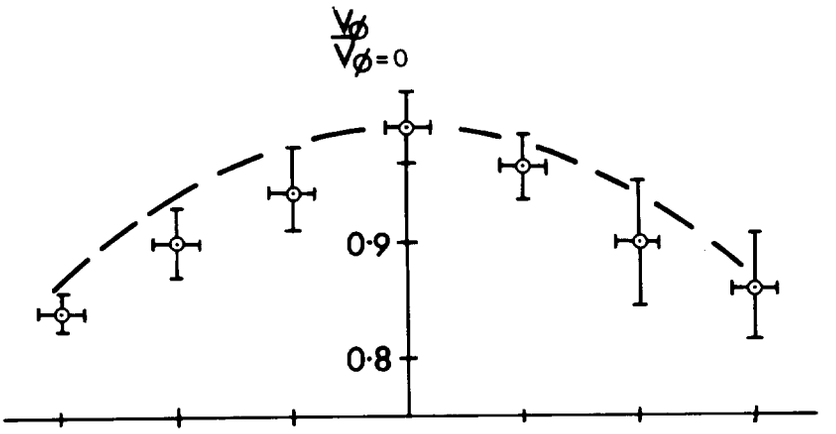

(d)

72cm/s

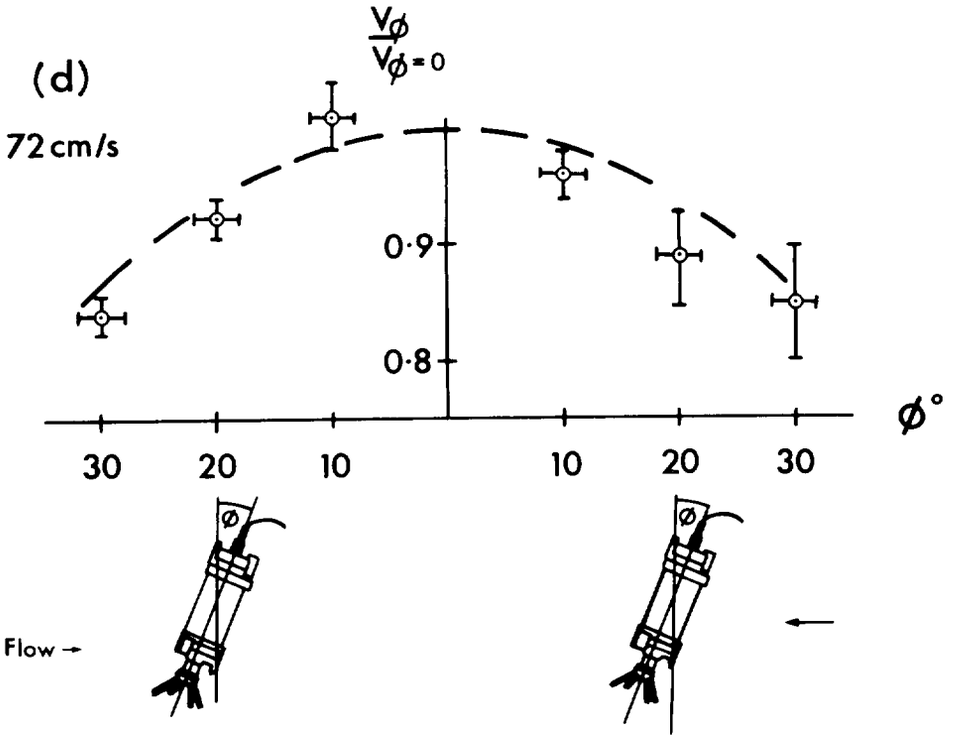

FIG. 12 C,D

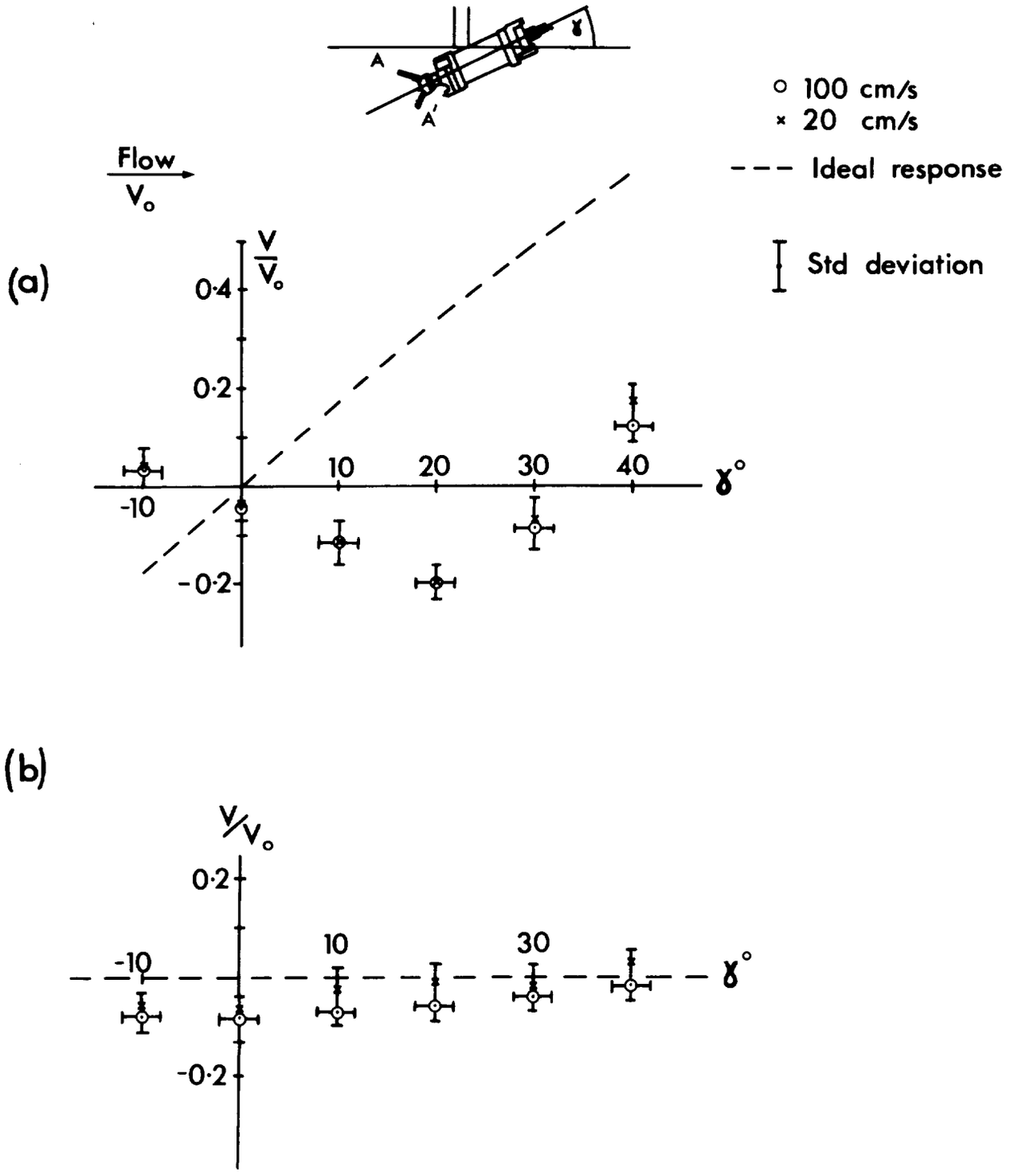

Fig.13 Response of current sensor tilted from horizontal position and towed at constant speed. Direction of motion lies in plane containing one pair of transducer support pillars AA'. Ideal response is shown by broken line. Note that standard deviation is for V only. 95% limits are typically ±0.01 in $\frac{V}{V_o}$; and uncertainty due to residual flow is <0.02 at 20cm/s, negligible at 100cm/s.

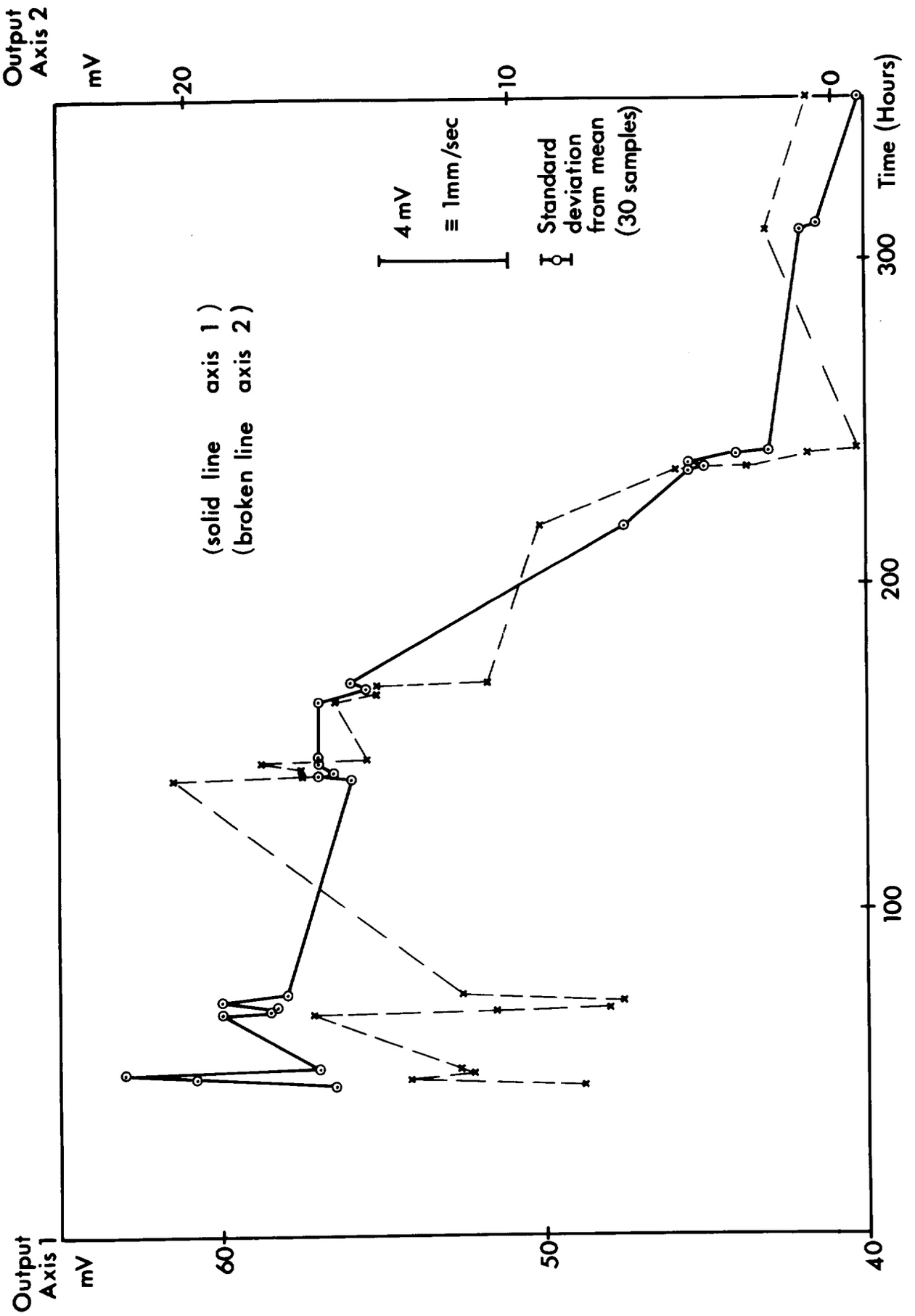

Fig.14 Variation of current sensor output with time in conditions of zero flow and constant temperature.

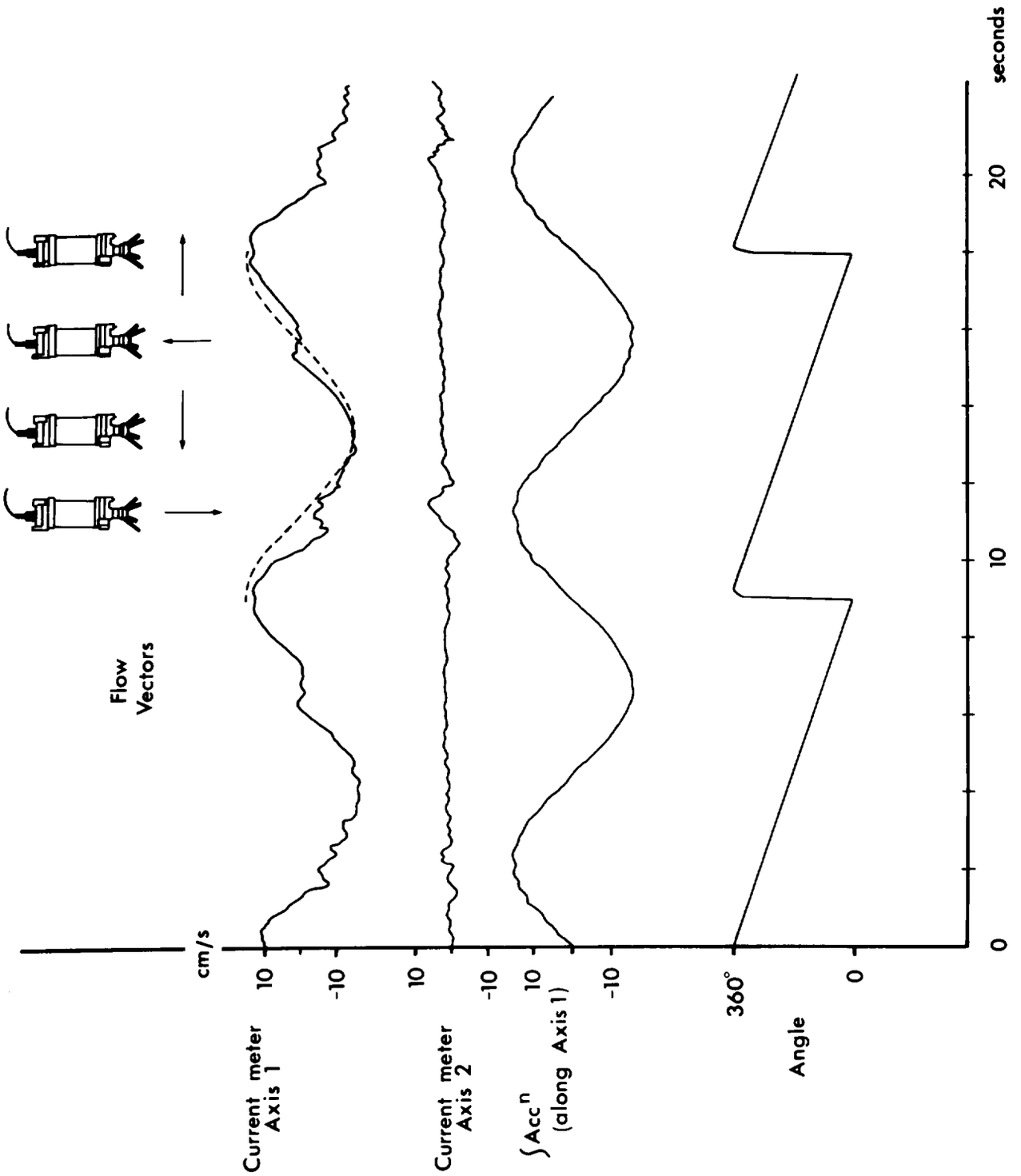

Fig.15 Outputs of vertically mounted current sensor and accelerometer (integrated) with time when moved in a vertical, circular path to simulate wave orbital motion.
Orbital diameter = 50cm
Period = 9 seconds
Ideal cosine response for current sensor shown by broken line.

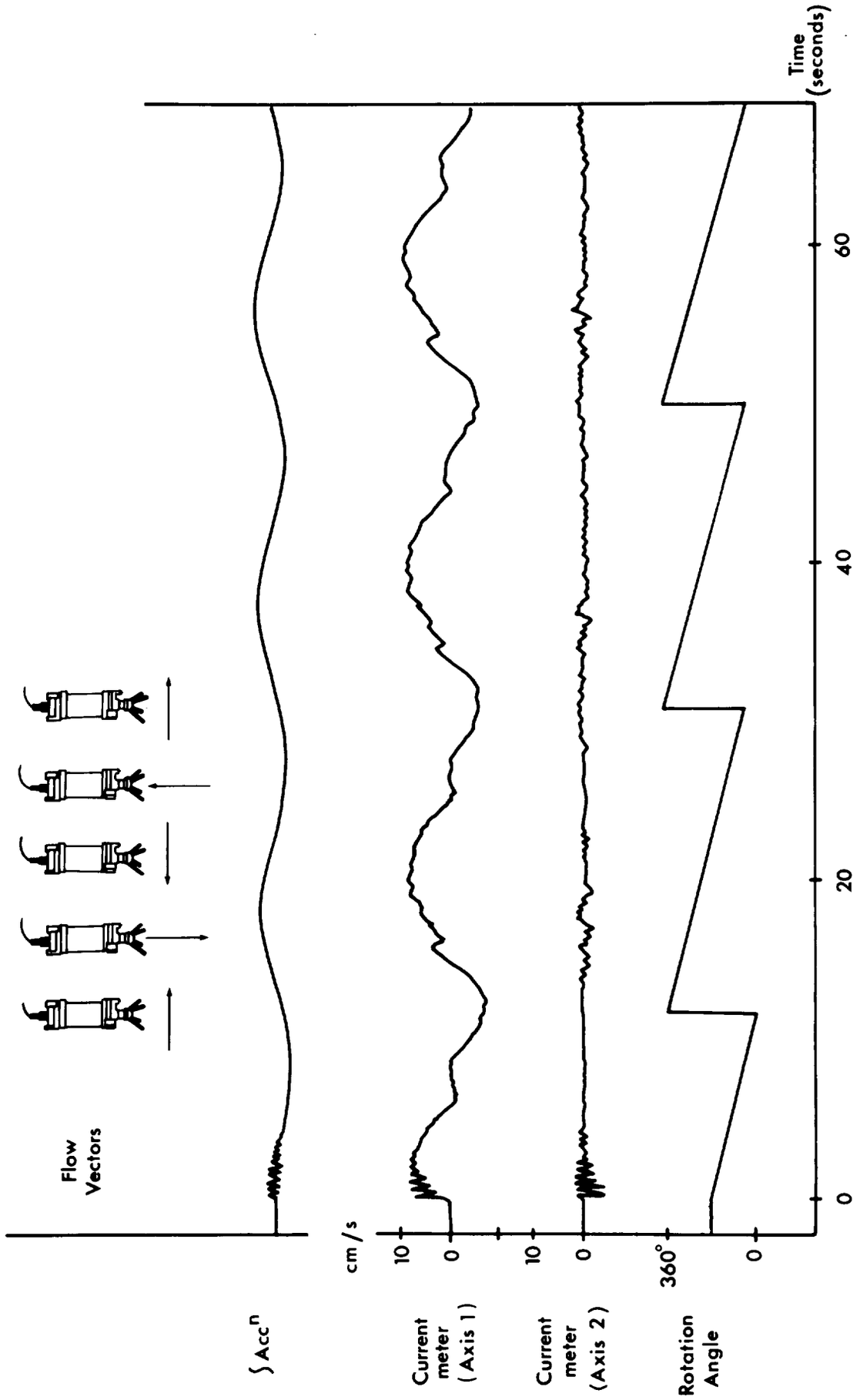

Fig.16 Outputs of vertically mounted current sensor and accelerometer (integrated) with time when moved in vertical, circular path to simulate wave orbital motion.
Orbital diameter = 50cm
Period = 19 seconds

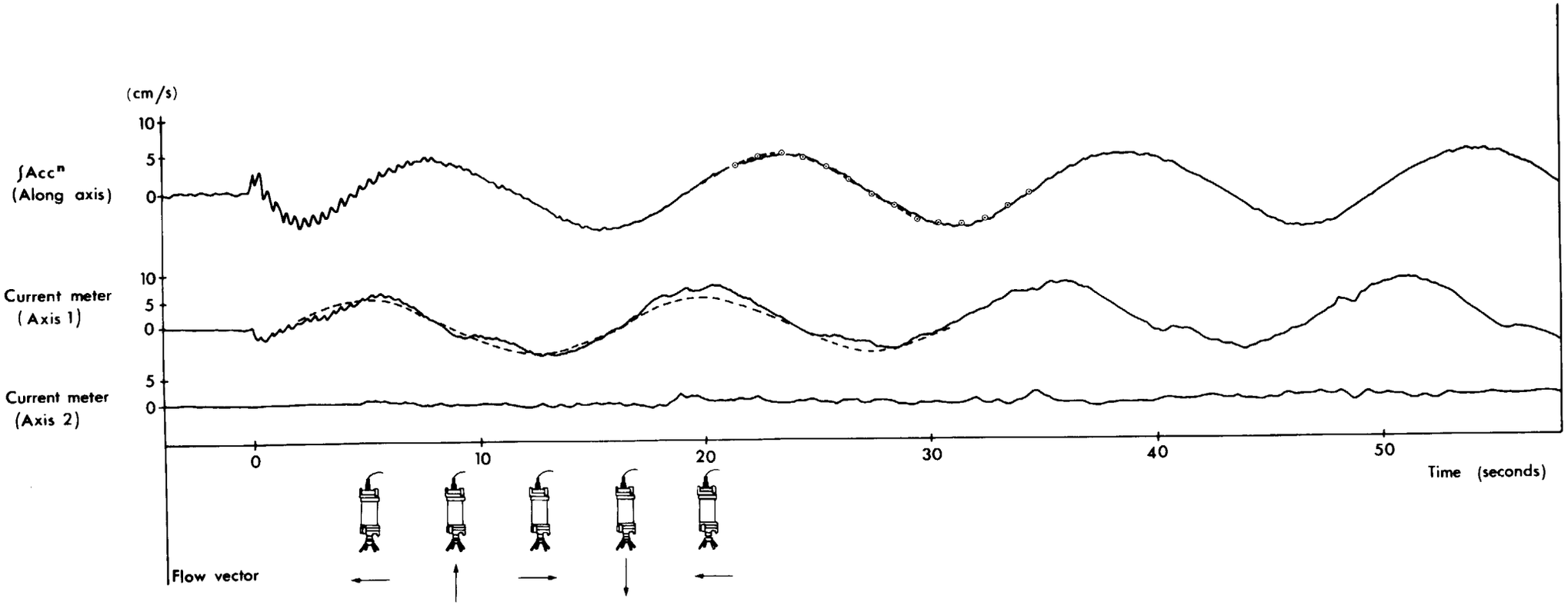

Fig.17 Outputs of vertically mounted current sensor and (integrated) accelerometer with time when moved in a vertical, circular path to simulate wave orbital motion.
Orbital diameter = 25cm
Period = 15 seconds
Broken line denotes ideal cosine response for current sensor.
Encircled points show slight departures from a uniform angular velocity.

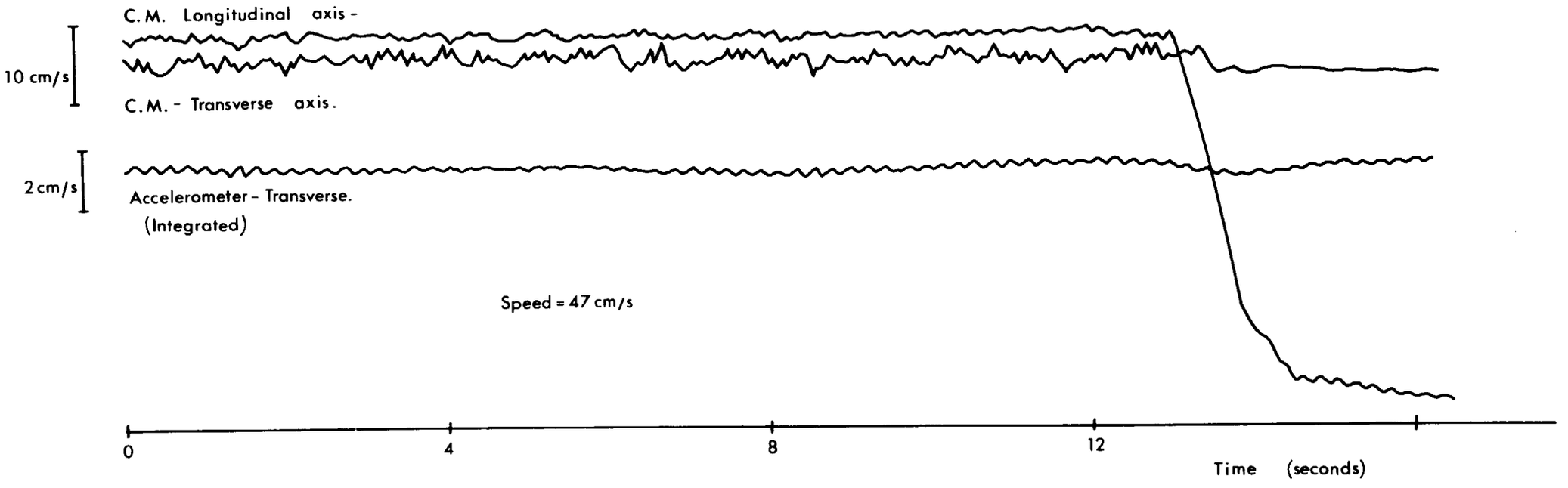

Fig.18 Typical output of current meter at constant speed. Carriage decelerates at t = 13 seconds. The accelerometer monitored transverse vibration in 5cm diameter support spar, which was of circular cross section. Axes aligned along and across tank.

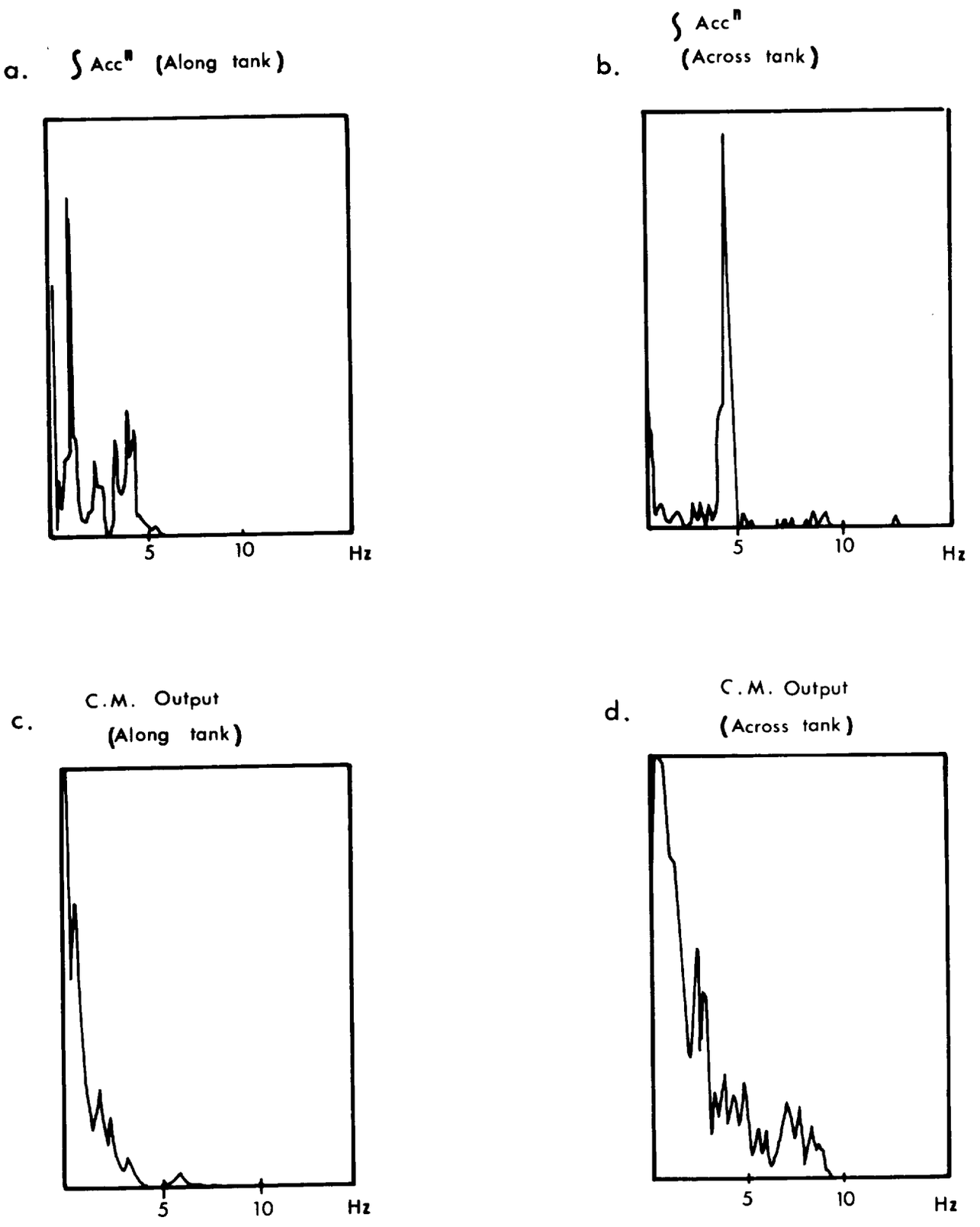

Fig.19 Spectra of current sensor outputs and vibration levels measured by accelerometers, in tow direction and across tank. Support spar was of streamlined section. Ordinates are linear. Speed - 35cm/s.

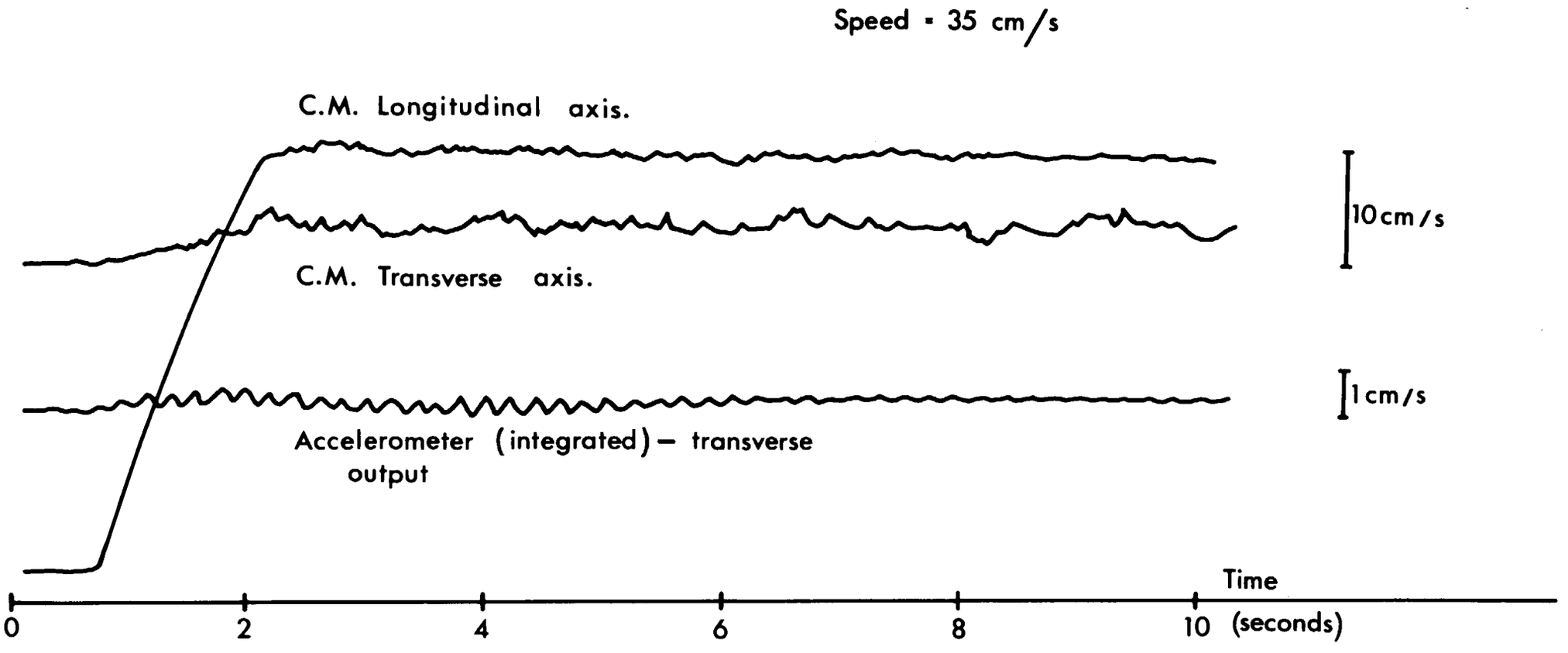

Fig.20 Typical output of current meter shown starting from rest. Axes aligned along and across tank. Accelerometer monitored transverse vibration in streamlined support spar.